

AD 739700

MECHANISM AND DETECTION OF  
DECOMPRESSION SICKNESS

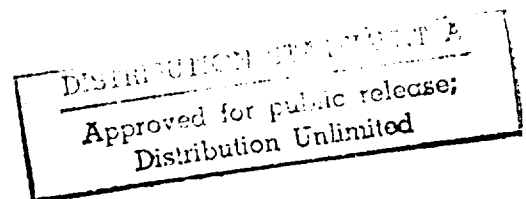
by

Michael R. Powell, Ph.D.

A Status Report to the  
Office of Naval Research  
Department of the Navy  
under  
Contract N00014-69-C-0346

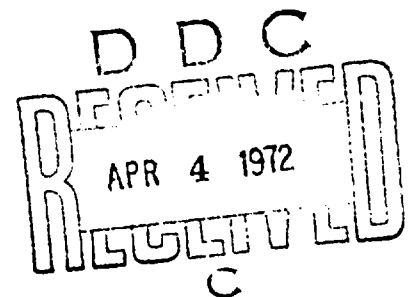
by

Reproduced From  
Best Available Copy



Ocean Systems, Incorporated  
Research and Development Laboratory  
Union Carbide Technical Center  
Tarrytown, N.Y. 10591

15 December 1971



Reproduction in whole or in part is permitted for any  
purpose of the United States Government.

# TABLE OF CONTENTS

	<u>Page</u>
I. SUMMARY	1
II. INTRODUCTION	3
III. ULTRASOUND PHYSICS	7
A. Nature of ultrasound waves	7
B. Attenuation of ultrasound	8
C. Pulsating bubbles	11
IV. ULTRASONIC MONITORING OF DECOMPRESSION	18
A. Doppler Ultrasound flowmeter	18
B. Pulsed echo	19
C. Acoustic-optical imaging	19
D. Through-transmission	20
V. EXPERIMENTAL METHODS AND RESULTS	22
A. Equipment	22
B. Experimental set up	27
C. Initial development	33
D. Lag Period	39
E. Treadmill studies and necropsy	43
F. Ultrasound Monitoring	49
G. Long term monitoring	49
VI. DISCUSSION	55
VII. REFERENCES	63

## LIST OF FIGURES

	<u>Page</u>
1. Theoretical bubble diameter at resonance <u>vs</u> frequency.	13
2. Attenuation coefficient <u>vs.</u> bubble radius for a frequency of 5.7 MHz.	16
3. Attenuation coefficient <u>vs.</u> frequency for a bubble of 4 micron radius.	17
4. "Main bang" (left) and the "peak" of the transmitted signal (right).	23
5. "Main bang", transmitted signal, and the electronic "gate" as it appears on the face of the CRT.	23
6. "Main bang" and the "peak" of the transmitted signal positioned within the electronic "gate".	23
7. Block diagram of the equipment used for the ultrasound attenuation experiments.	25
8. Plastic restraining cage used to hold the thigh muscles in position between the two 5.7 MHz ultrasound transducers.	28
9. Pressure chamber used for the compression/decompression studies.	29
10. Signal attenuation <u>vs.</u> pressure for a 5.7 MHz signal.	32
11. Per cent decompression hazard <u>vs.</u> time at 6 ATA in air.	33
12. Signal attenuation <u>vs.</u> time from start of compression.	36
13. Treadmill used to assess the degree of decompression sickness in the rat.	38
14. Bends score for each of 32 rats as a function of time from the start of decompression.	41
15. Attenuation of a 5.7 MHz signal measured across the thigh muscle as a function of time following start of decompression.	43
16A. Bubble detected visually in posterior vena cava <u>vs.</u> time after decompression.	45
16B. Individual bends score for two rats <u>vs.</u> time following start of decompression.	45
16C. Signal attenuation <u>vs.</u> time following start of decompression.	45
17. Working hypothesis indicating the location and pathological result of each of the three types of bubbles.	53

LIST OF TABLES

	<u>Page</u>
I. Acoustic Amplitude Absorption Coefficient	14
II. Scoring protocol for decompression sickness signs	40
III. Individual bends scores for various pressure exposures	40

Details of illustrations in  
this document may be better  
studied on microfiche

I. SUMMARY

This report describes our investigations of the use of ultrasound techniques for the study of mechanisms and detection of decompression sickness under Contract N00014-69-C-0346 between the Office of Naval Research and Ocean Systems, Inc. Other aspects of this contract dealing with miniature pig decompressions and computations of gas transport will be reported separately.

We employed a through-transmission technique of ultrasound detection of bubbles using a single frequency of ultrasound at 5.7 MHz. Heavy, male Wistar-strain rats were used as the biological system.

In this report we discuss the theoretical and experimental basis of through-transmission ultrasound detection of bubbles in a biological system and compare this method to Dobbler, pulsed-echo, and acoustic-optical imaging techniques. Specifically, we have followed ultrasound signal attenuation as a function of pressure and as a function of time during and following controlled decompression from depth (pressure) exposures. Measurements were made using the foot and also the thigh muscle of the rat as the site of detection.

The course of development of decompression sickness symptoms and of visible bubbles in the circulatory system were compared to ultrasonic signal attenuation measurements for similar decompression conditions. Animals were compressed in air to 6 ATA and decompressed at 2 atm./min. after variable exposure of 15-75 minutes at depth.

Parameters of ultrasound signal attenuations -- time to attain an effect, rate of change to maximum effect, magnitude of maximum effect, and time to recover the original signal -- paralleled the manifestation of corresponding parameters of decompression sickness symptoms. Visible intravascular bubbles, primarily in the venous system, were found in animals exhibiting a range of decompression symptoms from mild or none to severe or

death but were seldom seen after about one hour past decompression.

Arterial bubbles on the other hand, were often seen in animals which died from decompression and only occasionally in animals which survived.

These over-all results are consistent with a working hypothesis which considers bubbles to be a necessary and sufficient mechanism for the several pathophysiological manifestations of decompression sickness and death. Three bubble "types" differing in anatomic location and size are postulated as occurring sequentially: capillary bubbles in localized tissues, bubbles released into the venous circulation, and bubbles later entering into the arterial circulation. There appear to be two distinct phases or mechanisms of pathophysiological response to decompression: one primarily involving capillary bubbles and leading to pain and paralysis and the other involving arterial bubbles and leading to death. Bubbles may be seen in the venous system in the absence of observable signs of decompression sickness.

## II. INTRODUCTION

The etiology of decompression sickness has been a mystery since Robert Boyle (1670) first noted the signs in animals which he had subjected to a reduced pressure. The Bibliographical Sourcebooks of Hoff (1948, 1954) and Greenbaum and Hoff (1966) give a good historical picture of the development of ideas up to the recent past. The work of Bert (translation, 1943) did much to develop the "bubble hypothesis" at a time when other theories were more prevalent. However, the inability of this early hypothesis to explain all of the known problems of this malady led to the proposal of other mechanisms. End (1938) suggested that the agglutination of red blood cells was the primary factor with bubbles as only a secondary but complicating factor; platelet clumping has also been shown to be involved. Hemoconcentration was emphasized as an important factor in altitude decompression by Malette, et al. (1962), and heparin has since been shown to be effective in treating decompression sickness, perhaps by reducing lipid emboli (Barthelemy, 1963; Philp, et al., 1967; Cockett, et al., 1968).

In spite of the other hypotheses proposed, the bubble hypothesis is believed by most workers in the field to be essentially correct despite the lack of specific facts concerning origin of the bubbles and their site of action. Gersch and Catchpole (1951) pointed out evidence for intravascular bubbles as the primary agent in both altitude and hyperbaric cases. Nims (1951) proposed a physical theory wherein nerve endings were deformed by the growing bubbles such that when a certain distortion pressure was reached, pain would result. The location of these bubbles was thought to be extravascular, an idea also espoused later by Hills (1966).

The mechanism by which bubbles actually form in animals subjected to reduced pressures is still not known with any degree of certainty. Early studies by Harvey and co-workers (Harvey, 1951a, 1951b) and Blinks, Twitty and Whiteker (1951) showed that muscular activity was a predisposing factor to the formation of visible bubbles in animals. Recent work of Buckles (1968) has focused on the growth and resolution of bubbles in the microcirculatory system of the hamster cheek pouch.

The hypothesis that bubbles are primarily responsible for decompression sickness leads directly to questions of the exact role of these bubbles as the causative agent, and this has been a very hazy area where theories are concerned. For theories which place the blame on extravascular bubbles (Nims, 1951; Ferris and Engal, 1951; Hills, 1966), the area of action is somewhat specific, while for those theories utilizing circulating or intravascular bubbles the anatomic site is more vague. Basically the theories propose that bubbles formed in the blood stream circulate until lodged in some venous or arterial channel. There they block the flow of blood and possibly grow by diffusion (Hempleman, 1963), thereby deforming nerve endings and causing pain.

One of the ideas related to the bubble hypothesis is that of the metastable limit for bubble formation. First proposed by Haldane, (Boycott et al., 1908), and called the "Haldane method", it states that blood can tolerate a considerable degree of supersaturation without the formation of a separate gas phase, and furthermore that this supersaturation limit is more-or-less fixed. That is to say, below this limit bubbles will not form while above it there will be a phase separation. In recent models, this metastable limit is proposed to be different for various tissues and depends upon the tissue half-time (Workman, 1969).



Whether indeed the formation of bubbles never occurs below this limit has been a difficult question to answer, and most attempts to answer it have made use of x-rays. This method, however, is not very sensitive and is most successful only for the detection of pockets of gas. If indeed only small bubbles were involved, they could not be easily detected by the use of this method. After the analysis of certain dive profiles, Hills (1966) concluded that phase separation always occurs during decompression with today's commonly used tables, e.g., U.S. Navy Diving Tables, and that these tables merely control the size of the bubbles, an idea which had been expressed earlier (Behnke, 1951).

Although a model was never fully developed, there is a belief that bubbles can and do exist without the manifestation of decompression sickness. In a way not known, it is thought that their existence remains unnoticed, and hence they are given the name "silent" bubbles. Hempleman (1963) refers to them as a "tissue-bubble" complex and states that gas uptake and release in animals is not symmetrical (over time) because the bubbles impede the flow of blood through the tissue which was loaded with gas by uninhibited capillaries.

The concept that bubbles form when a metastable limit has been passed raises the question of why a delay time or "lag period" is often seen for the development of decompression sickness. If indeed bubbles do form when a limit has been exceeded, to a first approximation the symptoms should follow immediately or shortly thereafter. However, in man there is often a "lag period" of minutes or even hours after decompression begins before symptoms are noted (Nims, 1951). Indeed, for the case of altitude decompression sickness the symptoms sometimes are not noted until the fliers are descending to the ground.

A chief problem has thus been to determine the presence or absence of bubbles in decompressed subjects and the relationship of these bubbles to the signs and symptoms noted. In the past, the observation of bubbles has been confined to those visible in the major vessels, and great reliance has been placed upon these bubbles as the harbinger of disaster. But there is also a dichotomy in that bubbles could not always be found upon autopsy. However, it has been believed that perhaps only a few small bubbles could be responsible for the problems of decompression sickness and now, of course, the problem is more complex since small bubbles presumably are harder to find visually than very large ones. This is especially true if one looks in the circulatory system of muscle tissue and not in the great vessels.

What is needed, therefore, is a method whereby a tissue can be interrogated to determine if bubbles are present. More specifically, we would like to know something about their time of appearance, number, size, and the duration of residence in the tissue. Ultrasound methods have some characteristics which make them suitable to provide answers to these questions, and these are described in more detail in the section which follows.

### III. ULTRASOUND PHYSICS

#### A. Nature of Ultrasound Waves

Sound waves, as distinct from electromagnetic waves, are matter waves and as such involve the rapid translocation of atoms or molecules. The frequency at which this motion takes place is in the range of 20 to 20,000 Hz for those sounds which are detectable by the normal human ear. Above the frequency of 20,000 Hz lies the region of "ultrasound", and the upper limits of this are traditionally placed at about  $10^9$  Hz. For medical diagnostic work, in which ultrasound is used for tissue visualization, the frequencies used are on the order of  $10^6$  Hz.

While the physical properties of audible (sonic) and ultrasound waves are the same, ultrasonic frequencies have some advantages in that:

- (1) they are highly directional,
- (2) they can be easily focused,
- (3) their shorter wave lengths make them useful  
for examining small structures, and
- (4) their higher frequencies can be used for investigating physical phenomena with short time constants; this specifically includes scattering of sound waves by pulsating bubbles whose radii are on the order of microns.

All medical diagnostic work involves the use of low intensity ultrasound. This is contrasted with higher intensities as would be employed in ultrasonic heating of tissues or in ultrasound surgery.

Sound waves can be described in terms of their frequency and wave length. As mentioned previously, the range of ultrasonic frequencies is from  $2 \times 10^4$  to  $10^9$  Hz. The principal waves in fluid systems are of the type known as longitudinal waves. The source of the vibrations moves in a direction which is parallel to the direction of the travelling wave, and the particles themselves which carry the wave undergo motion which is parallel to the direction of the wave. A continuous pattern of compression and expansion is found. In systems with a high viscosity and in solids, transverse, or shear, waves are also found to occur. In this case, the direction of the wave travel is perpendicular to the direction of the particle motion. For biological systems, transverse waves are found to occur only in bone.

The wave length is a function of the speed of the matter wave in the propagation medium and the frequency. This length is given by the formula

$$\lambda = c/f$$

where  $\lambda$  is the wave length,  $c$  is the wave velocity, and  $f$  is the frequency. The wave length for a  $10^6$  Hz wave in water is 1.4mm. For biological studies involving tissue, the velocity of sound in water ( $1.4 \times 10^3$  m/sec) is normally used for purposes of calculation.

#### B. Attenuation of Ultrasound

It is of value to examine in some detail the various mechanisms by which the attenuation of an ultrasound beam can occur.

A sound wave passing through a medium -- solid, liquid or gas -- is reduced in intensity according to the formula

$$I = I_0 e^{-2\alpha x} \quad (1)$$

where  $I$  is the intensity,  $x$  the distance traveled, and  $\alpha$  is the amplitude

absorption coefficient. The classical, or Stokes-Kirchoff, absorption coefficient is given by

$$\alpha_{\text{class}} = \frac{8\pi^2 f^2}{3 v \rho} \left[ \eta + \frac{3}{4} \left( \frac{C_p - C_v}{C_p C_v} \right) K \right] \quad (2)$$

where  $f$  is the frequency,  $v$  is the velocity,  $\rho$  is the density,  $\eta$  is the viscosity,  $K$  is the heat conductivity, and  $C_p$  and  $C_v$  are the specific heats. The absorption coefficient for water agrees quite well with the value calculated by this equation. The coefficient for water is about  $20 \times 10^{17}$  ( $\text{sec}^2/\text{cm}$ ) while for air it is about 1000 times larger in that although  $\eta$  is 50 times smaller for air than water,  $v$  is  $4 \frac{1}{2}$  times smaller and  $\rho$  is 1000 times smaller. The pressure dependence of the absorption coefficient of water is very small (Litovitz and Carnevale, 1955).

The intensity of sound waves passing through an interface is given by the transmission coefficient  $\alpha_t$  and is defined as the ratio of the intensity of the transmitted wave to the intensity of the incident wave. For a plane wave incident at right angles to a plane boundary separating media of acoustic impedances  $\rho_1 c_1$  and  $\rho_2 c_2$  where  $\rho$  is the density and  $c$  is the speed of sound in the medium, the transmission coefficient  $\alpha_t$  is given by:

$$\alpha_t = \frac{4\rho_1 c_1 \cdot \rho_2 c_2}{(\rho_1 c_1 + \rho_2 c_2)^2} \quad (3)$$

Because of the large differences in acoustic impedance between liquids and gases, almost no transmission takes place at a liquid-gas interface, and hence gas "pockets" will greatly attenuate an ultrasound wave.

Muscle movement brings different tissue interfaces into the ultrasound beam which results in a change of the baseline attenuation. A shift of angle between the interface and the incident beam will also change the strength of the transmitted signal. For this reason, muscle movement

artifacts must be eliminated as they can be responsible for large distortions in the reflection-transmission pattern as measured on the detection instruments.

For the case where the sound is attenuated by small objects in a liquid medium, an important factor is scattering. Scattering can be divided into three classes:

- (1) when the body has dimensions which are much larger than a wave length, specular reflection occurs and an "acoustic shadow" is produced (this is the case treated above),
- (2) when the object is comparable in size to a wave length of sound, scattering and diffraction phenomena both occur, and
- (3) when the object is small with respect to a wave length, scattering occurs but the attenuation is reduced greatly.

The equations for scattering have been developed for the case of the sphere and the cylinder (Gobberman, 1968). The intensity  $I_{r\phi}$  of the radiation scattered from a cylinder of radius  $r_0$  measured at an angle  $\phi$  with respect to the incident radiation and at a distance  $r$  is given by the equation:

$$I_{r\phi} = I_0 \frac{\pi r_0}{8 r} (\beta r_0)^3 (1 - 2 \cos \phi)^2 \quad (4)$$

when  $\beta r_0 \ll 1$

where  $I_0$  is the incident intensity, and  $\beta = 2\pi/\lambda$ , where  $\lambda$  represents wave length. For the case of a spherical body, the scattered intensity is

$$I_{r\phi} \approx 0.11 (\beta r_0)^4 (r_0/r)^2 (1 - 3 \cos \phi)^2 \quad (5)$$

when  $\beta r_0 \ll 1$

The most important aspect for the case of attenuation is the total scattering

power  $W_s$ ; for the cylinder, this is given by the equation

$$W_s \approx 7.5 (\beta r_o)^3 r_o I_o \quad (6)$$

and for the sphere

$$W_s \approx 5.6 (\beta r_o)^4 r_o^2 I_o \quad (7)$$

where for both cases,  $\beta r_o \ll 1$ . Thus equations (6) and (7) hold best for situations where  $\beta r_o \ll 1$  or the diameter  $\approx 8\mu$  where the radiation is at 5.7 MHz. The scattering cross-section, the ratio of scattered intensity to incident intensity, goes as the fourth power of the radius for a sphere ("Rayleigh scattering") and the third power of the radius for the cylinder. When  $\beta r_o \gg 1$  (diameter  $\approx 0.8$  mm), the scattering cross-section is the same for the sphere and the cylinder and is equal to twice the geometric cross-section.

For the cases in which ultrasound attenuation is used for bubble detection in living systems, it is necessary to insure against changes in signal attenuation by changes in the mechanisms indicated above. Attenuation by the development of a gas phase should be the only process occurring to reduce the ultrasound beam intensity. Unquestionably, movement of the animal, with a resulting movement of tissues and interfaces, must be avoided if a stable base line is to be maintained.

### C. Pulsating Bubbles

The presence of a gas phase in a liquid causes a marked attenuation of an ultrasound beam passing through it. Bubbles of a given size are found to pulsate under the influence of periodic oscillations of the surrounding medium. The idea of a "resonant frequency" in a gas bubble suspended in a liquid phase was first used by Minnaert (1933) to explain the sound generated by running water in streams. He developed an equation relating the bubble size to the sound frequency; this frequency  $f$  is given by

$$f = \frac{1}{2\pi R_0} \left( \frac{3\gamma P_a}{\rho} \right)^{1/2} \quad (8)$$

where  $P_a$  is the ambient pressure,  $R_0$  is the radius,  $\rho$  is the liquid density, and  $\gamma$  is the ratio of specific heats for the gas in the bubble ( $\frac{C_p}{C_v}$ ). In an attempt to explain cavitation damage, Smith (1935) developed a similar equation for bubbles oscillating in a sound field. His equation took into account the effect surface tension would have on very small bubbles. The "resonant frequency" is thus given by

$$f = \frac{1}{2\pi R_0} \left[ \frac{3\gamma(P_a + 2S/R_0)}{\rho} \right]^{1/2} \quad (9)$$

where  $S$  is the surface tension. The resonant frequency for air bubbles in water at 1 atm as a function of their diameter is shown in Figure 1.

The modes by which pulsating bubbles dissipate acoustic energy has been studied theoretically by Devin (1959); he lists these modes as thermal, radiation, and viscous. The acoustic amplitude absorption coefficient  $\alpha$  is dependent upon these three modes (Fry and Dunn, 1962; Dunn, et al., 1969) and the relative importance of each mode will depend on the characteristics of the total system.

The acoustic amplitude absorption coefficient is given by equation 10.

$$\alpha = \frac{bNu}{l} \left[ \frac{\frac{3\gamma P_a}{R_0^2} + W^2 \rho}{\left[ \frac{1}{4\pi R_0} \left( W^2 \rho - \frac{3\gamma P_a}{\epsilon R_0^2} \right) \right]^2 + b^2 W^2} \right] \quad (10)$$

Meanings and numerical values of the terms are given in Table I. Calculations show that, for the bubble size dealt with here, i.e., on the order of microns, the numerical values of  $g$  and  $\epsilon$  are approximately equal to 1. In addition, the thermal dissipation parameter is small with respect to the radiation and viscous dissipation parameters. For the case of 5.7 MHz, the equation is



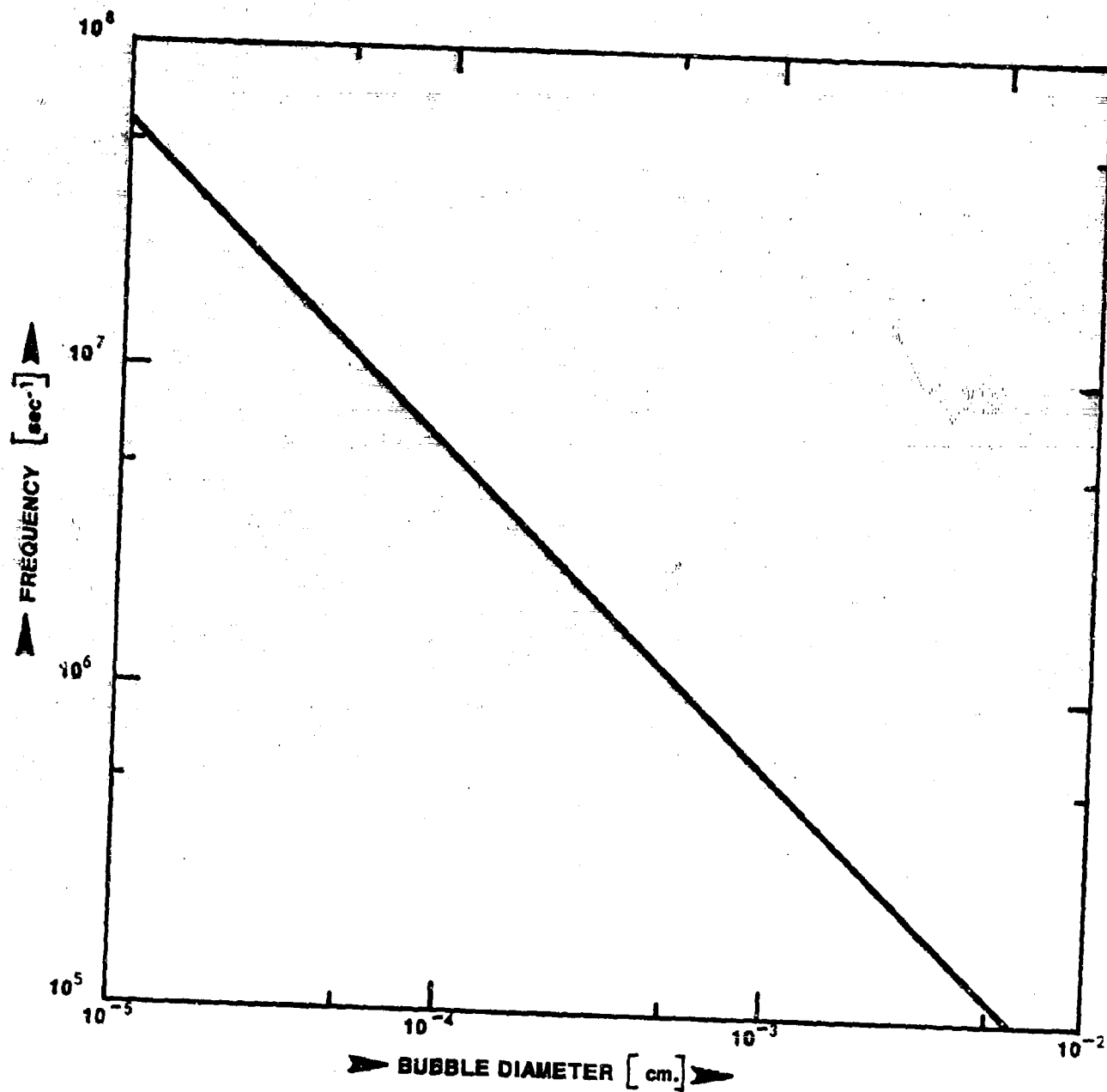


Figure 1. Theoretical bubble diameter at resonance vs. frequency.  
Calculated for air bubbles in water at 1 ATA.

solved for the total acoustic amplitude absorption coefficient in Figure 2. The units of  $\alpha$  are nepers per centimeter of path length for a unit bubble density per  $\text{cm}^3$ . (A neper is the Napierian equivalent of a decibel and equals 8.7 db.). It can be seen that large bubbles dissipate more ultrasound energy, and that large dissipations occur at the "resonant frequency".

To solve this equation, we assume that the gas phase is in the form of a sphere and does not contact any medium other than blood plasma. Obviously this cannot hold true for bubbles with a radius greater than 4 microns in the capillaries for these would then touch the capillary walls and assume a cylindrical shape. The bubbles are assumed suspended in plasma and do not contact the corpuscles.

Equation 10 can be rewritten, if  $g/c$  is approximately equal to 1, in terms of the "resonant frequency",  $W_0$ . We have thus,

$$\alpha = \frac{bNv}{4} \left[ \frac{W_0^2 p + W_p^2}{\left[ \frac{1}{4\pi R_0} (W_p^2 - W_0^2 p) \right]^2 + b^2 W^2} \right] \quad (11)$$

The equation is at a maximum when  $W$  is equal to  $W_0$ ; this is shown graphically in Figure 3 for a bubble with a radius of 4 microns. By means of ultrasound transducers which are operated outside of their range of resonance, it should be possible to scan a frequency range and determine the radii of tissue bubbles by observing the frequency at an absorption maximum. This would form an "acoustic spectrogram"; this technique has been applied by Richardson (1958) to the problem of residual nucleation sites and cavitation. If indeed there were a class of bubbles with a given radius responsible for the problems of decompression sickness, this technique of the "acoustic spectrogram" would allow one to determine which frequency for ultrasound monitoring would be most sensitive for a premonitory detection system in human divers.

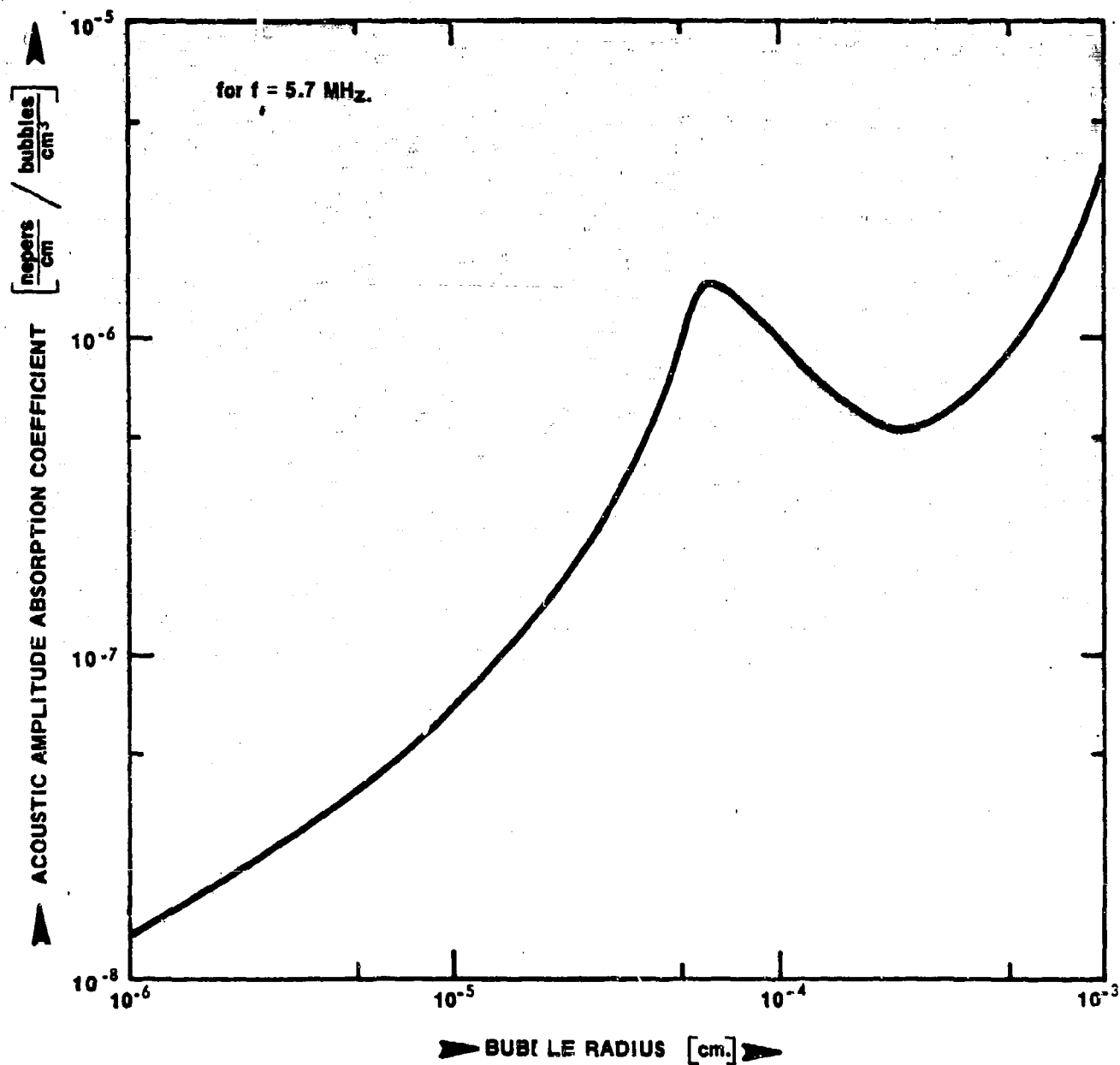


Figure 2. Attenuation coefficient vs. bubble radius for a frequency of 5.7 MHz. Calculated for air bubbles in plasma at 1 atm. The peak occurs at a bubble radius of about 0.6 microns.

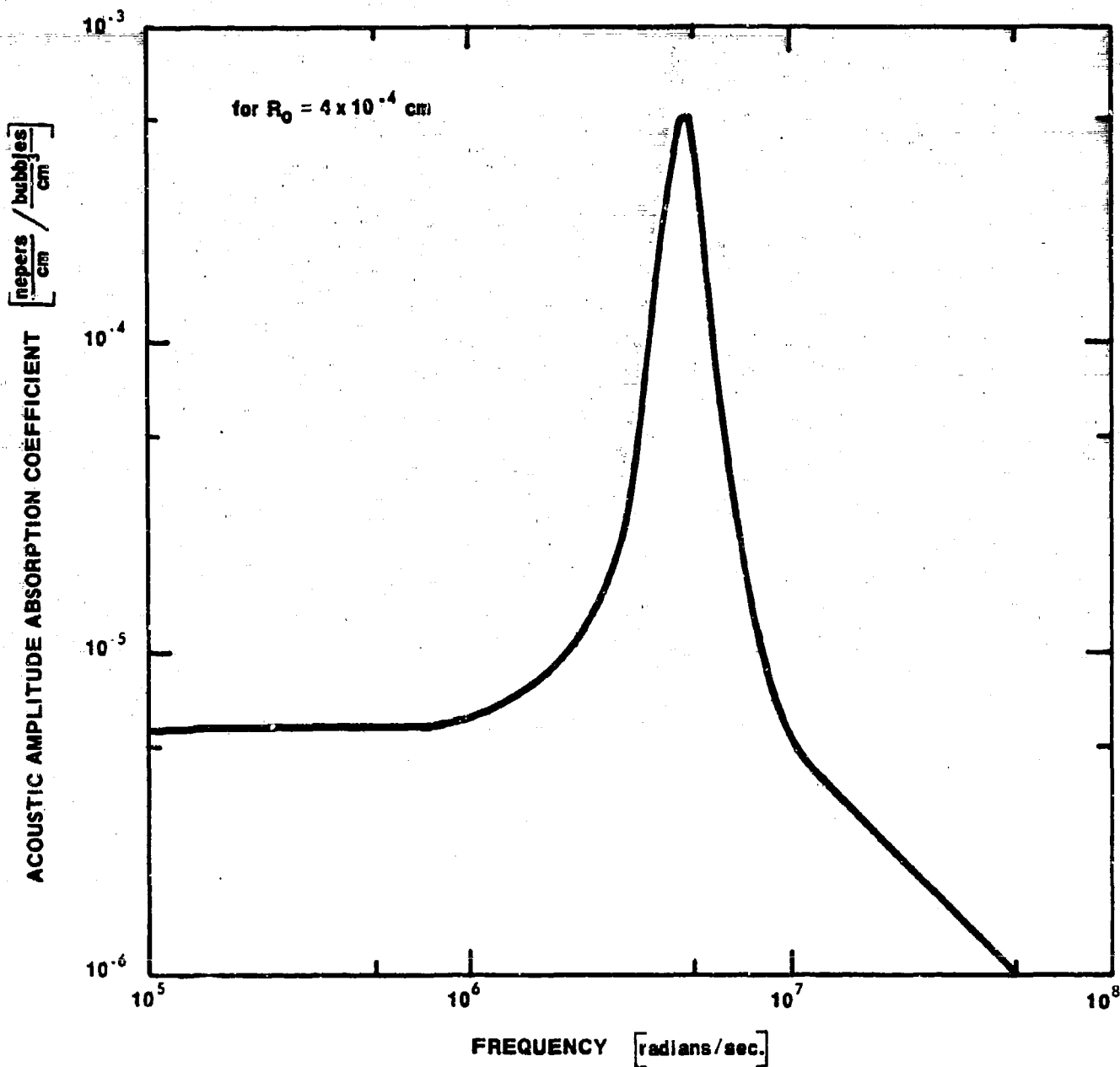


Figure 3. Attenuation coefficient vs. frequency for a bubble of 4 micron radius. Calculated for air bubbles in water at 1 ATA. The peak is at slightly less than 1 MHz.

TABLE I

Acoustic Amplitude Absorption Coefficient

$$\alpha = \frac{b N v}{4} \left\{ \frac{\omega_0^2 \rho + \omega^2 \rho}{\left[ \frac{1}{4 \pi R_0} (\omega^2 \rho - \omega_0^2 \rho) \right]^2 + b^2 \omega^2} \right\}$$

Quantity	Definition	Numerical Value
$\omega_0$	$\frac{1}{R_0} \left\{ \left( \frac{3 r P_0}{\rho} \right) \left( \frac{9}{\epsilon} \right) \right\}$ angular resonant frequency of bubble	e.g. 10 micron diameter is $10^5 \text{ sec.}^{-1}$
$g$	$1 + \frac{2 \sigma}{P_0 R_0} \left( 1 - \frac{1}{3 h} \right)$	approximately = 1
$\epsilon$	$1 + \frac{3(r-1)}{2 \frac{1}{2} R_0} \left\{ 1 + \frac{3(r-1)}{2 \frac{1}{2} R_0} \right\}$	approximately = 1
$\phi$	$\left( \frac{\omega_0 \rho g C_p}{2 K} \right)$	
$v$	acoustic velocity in water	$1.5 \times 10^5 \text{ cm/sec}$
$\gamma$	ratio of specific heats of air	1.4
$P_0$	static pressure	$10^6 \text{ dyne/cm}^2$
$\rho$	density of plasma	$1.0 \text{ g/cm}^3$
$\rho_g$	density of air	$1.29 \times 10^{-3} \text{ g/cm}^3$
$\sigma$	surface tension of water	75 dyne/cm
$h$	$\gamma/\epsilon$	$1 < h < \gamma$
$C_p$	heat capacity at constant pressure of air	0.24 cal/g
$K$	thermal conductivity coefficient of air	$5.6 \times 10^{-6} \text{ cal/cm sec}^\circ \text{C}$
$\eta$	viscosity of plasma	$3.2 \times 10^{-2} \text{ poise}$
$N$	number of bubbles per unit volume	
$b$	total dissipation parameter, $b_t + b_r + b_v$	
$b_t$	thermal dissipation parameter	very small
$b_r$	radiation dissipation parameter, $\frac{\rho \omega^2}{4 \pi v}$	$6.9 \times 10^8 \text{ g/cm}^4\text{-sec}$
$b_v$	viscous dissipation parameter, $\frac{\eta}{\pi R_0^3}$	
$R_0$	radius of gas bubble	
$\omega$	angular frequency of sound field, $2 \pi f$	$3.58 \times 10^7 \text{ radians/sec}$ (at 5.7 MHz)

### III. ULTRASONIC MONITORING OF DECOMPRESSION

#### A. Doppler Ultrasound Flow meter

While the through-transmission technique has been the method employed in this study, it is by no means the only technique available for decompression sickness studies using ultrasound waves. At the present time, most work has been done using the Doppler ultrasound flowmeter. This device, developed by Franklin, Schlegel, and Rushmer (1961) for blood flow measurement, was first employed for bubble detection by Gillis et al. (1968a, b) and Spencer and Campbell (1968). The blood flowmeter detects moving particles (blood cells or bubbles) by measuring the frequency (Doppler) shift of an ultrasound wave scattered from the moving particles. In its use as a flowmeter, it was found to be very sensitive to small moving gas bubbles. Recent work by Smith and Spencer (1970) has shown the presence of bubbles in the posterior vena cava of sheep before the onset of symptoms. However, the bubbles have also been found in sheep which, when subjected to marginal decompression, did not show signs of decompression problems.

The device gives an indication of bubbles which may have been formed at any point in the body and the results have been difficult to interpret in a practical way. At present, there is no proof that bubbles in the venous pool are associated with decompression sickness, and, indeed, our study leads us to believe that their presence is to be expected irrespective of the development of distress following a decompression. Furthermore, using the Doppler instrument it is impossible to detect stationary bubbles, and these, if caught in the microcirculatory system, may be the true factors responsible for the disease.

For many uses of the Doppler ultrasound technique, it is necessary to implant the transducers surgically. This is a complicated procedure and is not completely suitable where human divers are concerned. It is, however, possible to use it in the transcutaneous mode for some vessels, and this has been done in some trials with human divers.

#### B. Pulsed Echo

The detection of echos from bubbles was attempted by Sutphen (1968) with a moderate amount of success. In observing the signal produced when rabbits and dogs were injected with air, he found that reflections from bubbles appeared as small "peaks" on the oscilloscope face. Because they were injected, the bubbles were quite large in terms of what one often finds in decompression sickness. The method was unfortunately not tested on animals which had just undergone decompression.

Perhaps the most difficult part of the echo method of bubble detection is an interpretation of what it is that one is seeking. Only in the most obvious cases, e.g., the eye, the brain, and the heart, has a good interpretation of echo patterns been made. Anyone who has observed the many reflections found in the human arm understands the difficult job it would be to see evidence of newly appearing echos. Furthermore, the echo pattern is extremely sensitive to muscle and transducer movement.

#### C. Acoustic-optical Imaging

Tissues can be visualized by interacting an ultrasound beam with a converging laser beam at right angles to each other. In passing through the fluid medium which is compressed and rarified by the sound waves, the light undergoes Bragg diffraction. If the ultra-

sound waves have been spatially modified by an object, an image of the object will be reconstructed by the light beam, and this can be viewed through a microscope. Buckles and Knox (1969) have tested the principle using hamsters and viewing the legs following decompression. Darkened areas indicate that a gas phase is forming in the leg tissue.

#### D. Through-transmission

Walder et al. (1968) showed that attenuation of a transmitted ultrasound beam could be effected by bubbles in tissues of an animal following decompression. Furthermore, the attenuation could be reversed and the signal restored to its original level by recompressing the animal. In vitro work was done by Manley (1969) in developing the through-transmission technique to detect bubbles in extracorporeal blood flow. We have reported its use to study the formation of bubbles in the legs of rats following decompression (Powell, 1971).

The through-transmission method possesses advantages in that both moving and stationary bubbles can be detected. It is able to monitor major vessels and the microcirculatory system in tissues, and indeed is capable of detecting intracellular bubbles. At this stage of knowledge of the etiology of decompression sickness, no bubble locus can be said a priori to be the cause of distress nor can any site be ruled out.

The instrumentation needed for this method is relatively simple, and the technique is easy to use. No surgical implantation is required, nor is it necessary to immerse the subject in water. The chief hinderance is that the subject must remain relatively still; for



rats this means that the limb under investigation must be mechanically restrained.

Placement of the transducers in a specific location allows one to interrogate certain muscle or tissue areas specifically. Unlike, for example, the Doppler flowmeter, it does not give information which is a "pooling" of data from all locations in the body. Such "pooled" information has proven difficult to interpret.

## V. EXPERIMENTAL METHODS AND RESULTS

This section describes our technique for measuring the attenuation of an ultrasound beam passing through the leg of a rat which has been held under pressure in a small chamber and subsequently decompressed.

### A. Equipment

The basic instrument used for generation and detection of the ultrasound waves was the UltraSonoscope, Model 101B, manufactured by Hoffrel Instruments Inc., Norwalk, Connecticut. This is a commercially available instrument sold to the medical profession. Ultrasound has been successfully used to non-invasively study numerous internal organs which are not easily observable by x-ray techniques such as the brain, or organs which are moving, for example, the heart. In addition, it has great value for the detection of small objects in the eye, or in the observation of the foetus which is sensitive to x-radiation.

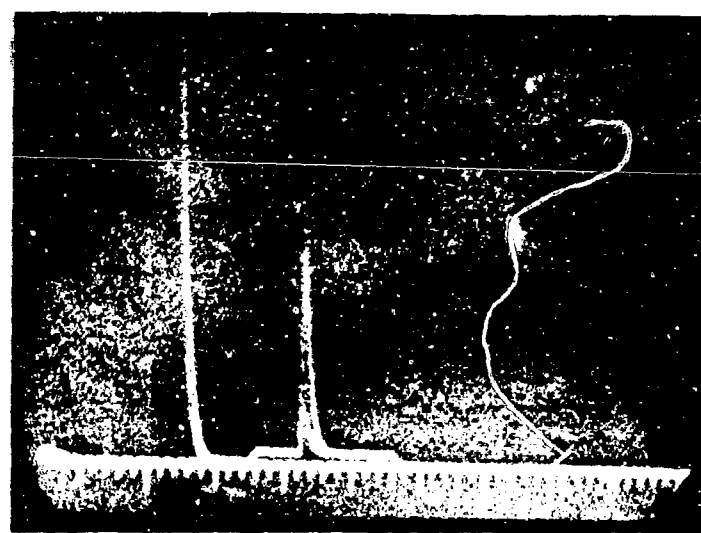
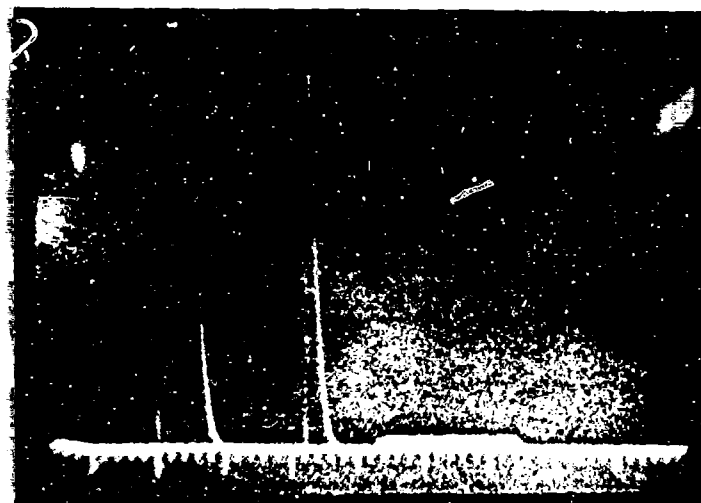
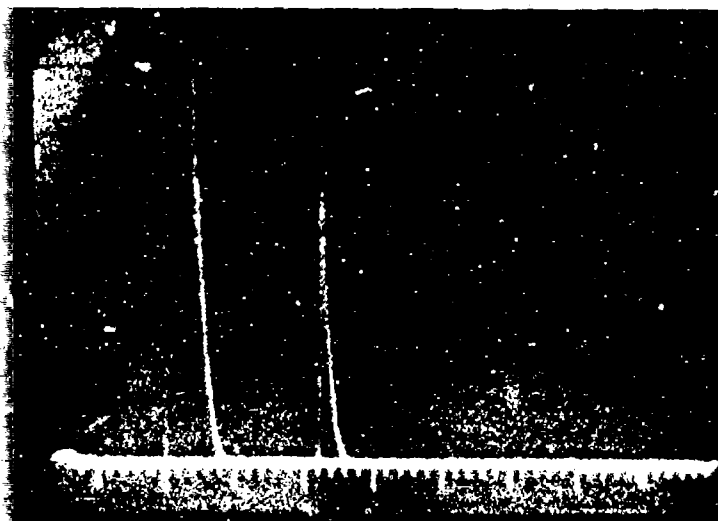
The beam power in all diagnostic equipment, including the Model 101 B, is of a very low level, typically on the order of 1 to 5 milliwatts/cm. The power level of equipment used in ultrasound physiotherapy is generally a few watts/cm. This latter value is below the pain level and about equal to the cavitation level; the power levels employed by the UltraSonoscope is thus about one one-thousandth of the energy needed for cavitation.

The ultrasound signals are generated by one transducer, pass through the tissue which is being interrogated, and are received by the second transducer. On the face of the oscilloscope of the UltraSonoscope, this received signal will appear as a "peak", in a manner similar to a sonar or radar "echo". Figure 4 shows the signal received by the second transducer after the signal has traversed an air gap; the first

Figure 4. "Main bang" (left) and the "peak" of the transmitted signal (right).

Figure 5. "Main bang", transmitted signal, and the electronic "gate" as it appears on the face of the CRT. Instrument is now in the Echotrol mode.

Figure 6. "Main bang" and the "peak" of the transmitted signal positioned within the electronic "gate". Instrument is in the Echotrol mode.



signal is the so called "main bang" produced by the signal generating transducer. Figure 5 shows the oscilloscope face as it appears when the instrument is operated in the Echotrol mode. A small rise or "gate" is seen next to the received signal "peak". This Echotrol feature is designed for use in echoencephalography when finding the midline of the brain. A feedback circuit causes the height of the midline "peak", when positioned within the movable electronic "gate", to remain essentially constant. This is of great benefit clinically where movement of the transducers, as they are held against the patient's head, causes a change in this "peak" height. Figure 6 shows the "peak" positioned within the "gate". The voltage needed to maintain a constant peak height can be measured at terminals B and G on the REMOTE connector at the rear of the instrument. Because of the Echotrol feature, an attenuation by bubbles will not effect a change in the peak height until the attenuation is beyond the ability of the instrument to compensate for the loss in signal.

By means of an attenuator box placed in-series between the receiving transducer and the UltraSonoscope, it is possible to calibrate the instrument and thereby measure signal attenuation in decibels. Attenuation of the signal by tissue bubbles can then be quantified. The range of the instrument is such that changes of attenuation of 40 to 45 db can be measured. The shielded transducer wires enter the chamber through a Conax (Conax, Buffalo, New York) pressure penetration. A block diagram of the equipment is shown in Figure 7.

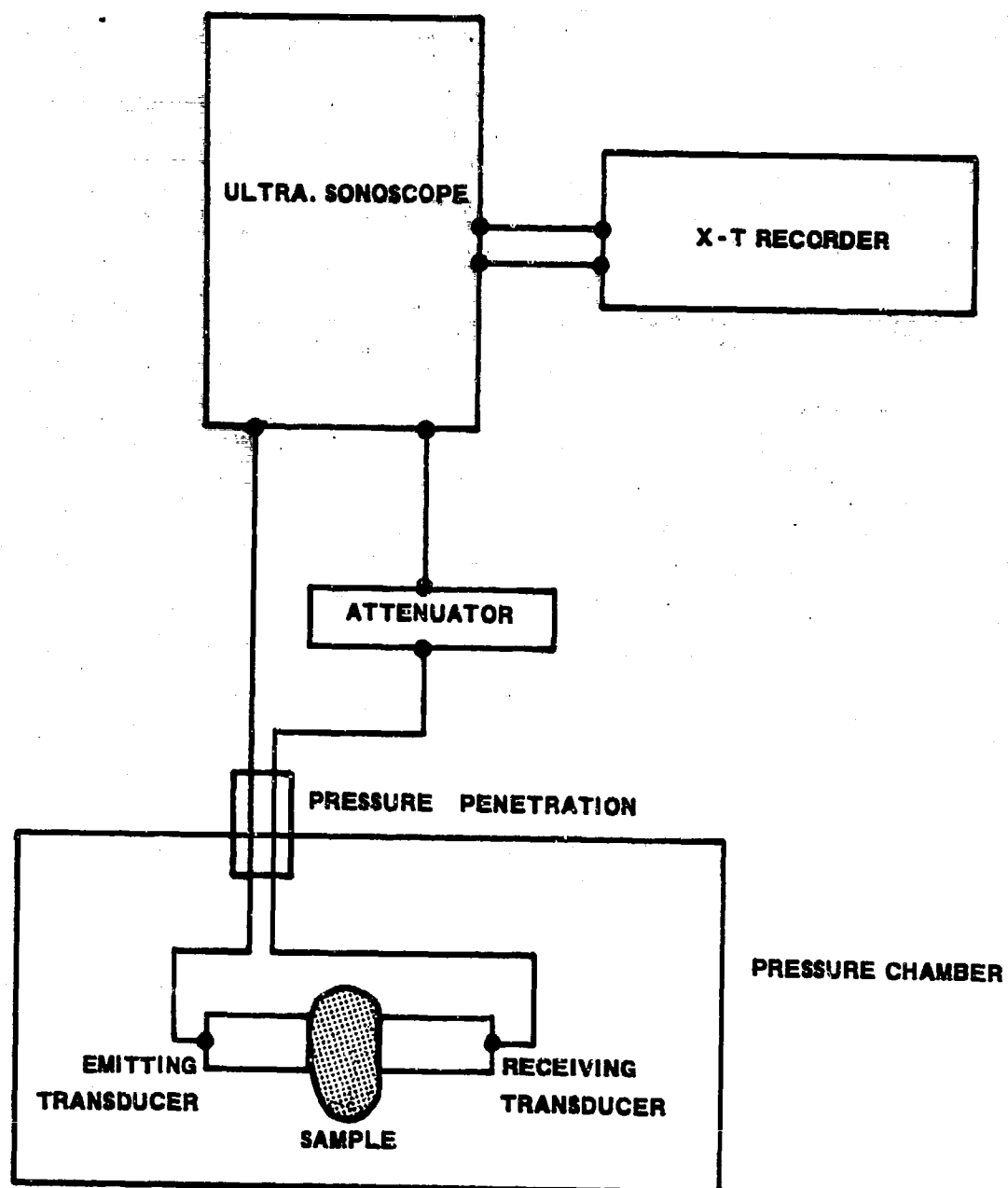


Figure 7. Block diagram of the equipment used for the ultrasound attenuation experiments.

#### B. Experimental Set up

For the successful operation of the equipment, it is necessary that the baseline of attenuation be stable. The transducers, once aligned, must not be allowed to move, and muscle movement must be kept to a minimum. For the first of these two criteria, various mechanical devices to hold the transducer could be used. For the experiments described here, the transducers were simply attached with hose clamps to a short metal bar. This we found provided sufficient alignment for the small inter-transducer distances encountered; the largest spacing used between the transducers was 1 1/2 cm for the rat thigh muscle. For cases requiring the removal of the transducer, or for human divers where larger inter-transducer spaces might be used, it would be necessary to construct a more rigid holder that would allow precise alignment of the transducers.

The most difficult problem encountered, and one not yet satisfactorily solved, involves muscle movement and the artifacts which it produces. This was partially solved, for the case of these experiments, by using tranquilizers and mechanical restraint. Initially the rats were anesthetized with Myothesia (SeMed Pharmaceuticals, Bristol, Tenn.). This drug is a combination of a muscle relaxant, Mephenesin, and a barbiturate, secobarbital. However, anesthetic drugs depress the animals respiration in such a way that they could exacerbate the effects of decompression.

It was later found that administration of the tranquilizing drug Acepromazine maleate (Ayerst Laboratories, Inc., New York, N. Y.) calmed the animal so that it would not struggle excessively. When used

in conjunction with a restraining cage which held the foot and thigh in position between the transducers, movement artifacts were almost completely eliminated. If the animal did struggle, and they did so occasionally, the tissue did not move from position to such an extent that the original signal level did not return after the movement. The restraining cage with the thigh and transducers in position is shown in figure 8.

Acoustic coupling between the transducers and the subject was made with silicone stopcock lubricant. This material provided good coupling without the tendency to run. Tests were made to show that bubble formation would not occur, during the decompression phase of the experiment, in this gel.

Compressions were carried out in a small pressure chamber, Figure 9, fitted with electrical and gas penetrations. The chamber was fitted with a window at one end to allow observation of the rat during and after decompression. This enabled one to observe the presence of leg movement between the transducers. The chamber was of a sufficient size that either one rat in a restraining cage with transducers or four rats in a partitioned cage could be decompressed at one time. The carbon dioxide was removed from the chamber by a small Baralyme (National Cylinder Gas, Chicago, Ill.) container through which air was moved with a small fan.

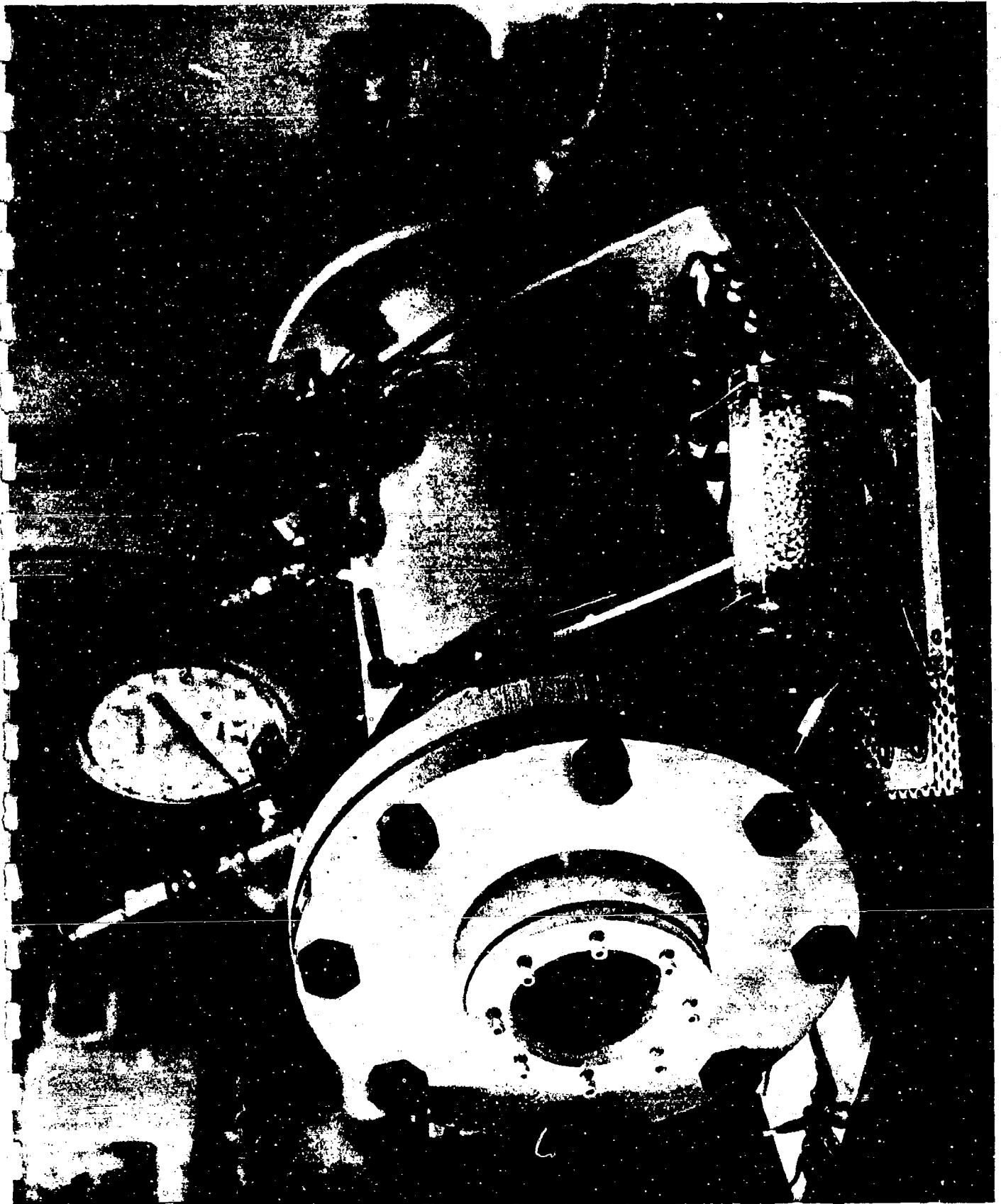
All pressurizations were made with compressed air. The compressions were continuous at a rate of approximately 5 atm/min.; the decompressions were continuous at a rate of exactly 2 atm/min. The



Figure 8. Plastic restraining cage used to hold the thigh muscles in position between the two 5.7 MHz ultrasound transducers.



Figure 9. Pressure chamber used for the compression/decompression studies. The glass window is seen at the left and the Baralyme scrubber, which has been removed from the chamber, is seen at the bottom center.



compressions were generally made to 6 ATA (1 ATA = 1 atm. abs., 760 mm Hg or 14.7 psi); the exceptions to this will be noted and occurred in the initial experiments to develop this method.

All experiments were performed using retired male breeders of the Wistar strain. They were in the weight range of 480 to 620 grams with an average of 550 grams and were given food and water ad libitum.

### C. Initial Development

Initial experiments to determine the applicability of the through-transmission technique were made by placing the foot or hand of a rat, anesthetized with Myothesia, between two 5.7 MHz ultrasound transducers. These initial experiments were recorded on an X-Y recorder plotting signal attenuation vs. pressure. Chamber pressure, the abscissa, was measured with a Statham pressure transducer while attenuation, the ordinate, was measured by the UltraSonoscope.

It was decided to investigate the limbs as this area of the body is most susceptible to decompression sickness. In addition, the hand and foot are convenient locations for transducer placement. The transducers were always arranged in "optical alignment", that is, so that the central axis of one passed through the central axis of the other. The "gate" on the UltraSonoscope was adjusted such that the second or third reflection fell within it. It was necessary to use a reflection in that the first through-pass signal and the tail of the "main bang" overlapped so much that resolution and positioning of the gate on earlier echoes was not possible. The use of reflections increased the sensitivity by increasing the path length, but it resulted in an increase in the magnitude of the movement artifacts.

All compressions were made with compressed air or nitrogen added to a chamber purged with oxygen. The same protocol was used for all of the trials, and it was developed so that each animal could serve as his own control. The experiments on each rat were made sequentially and on the same day. The results of one such experiment is shown in Figure 10. Line I was a compression to 2.7 ATA and a return to 1 ATA; this was made to check for the presence of "pressurization artifacts" and none over 2 to 3 decibels was found. Line II was a compression to 2.7 ATA, a hold for 15 minutes and decompression to 1 ATA. This condition is a mild profile, seen in Figure 11, and produced no attenuation changes. A recompression, Line III, to 6 ATA, holding for 60 minutes, and decompression to 1 ATA resulted in an attenuation of the signal after reaching the surface and with a lag time in various trials of from 15 seconds to 2 minutes. In this particular experiment, a 14 decibel attenuation was found and the animal exhibited respiratory distress. It was quickly recompressed to 2.7 ATA with oxygen and further compressed to 6 ATA with nitrogen; the signal strength returned to its pre-decompression intensity. The return of the signal to its initial pre-decompression intensity is interpreted as evidence that attenuation is caused by bubble formation.

This compression-decompression protocol was used on 17 different rats, and this type of response was found in 15. No significant difference could be found between the responses of transducers on the hind foot as compared with the forefoot. While this system could

Figure 10. Signal attenuation vs. pressure for a 5.7 MHz signal.  
Ultrasound probes placed on the hand of the rat. "Bottom  
time" for Line I is 0 minutes, for Line II it is 15 minutes,  
and for Line III it is 60 minutes.

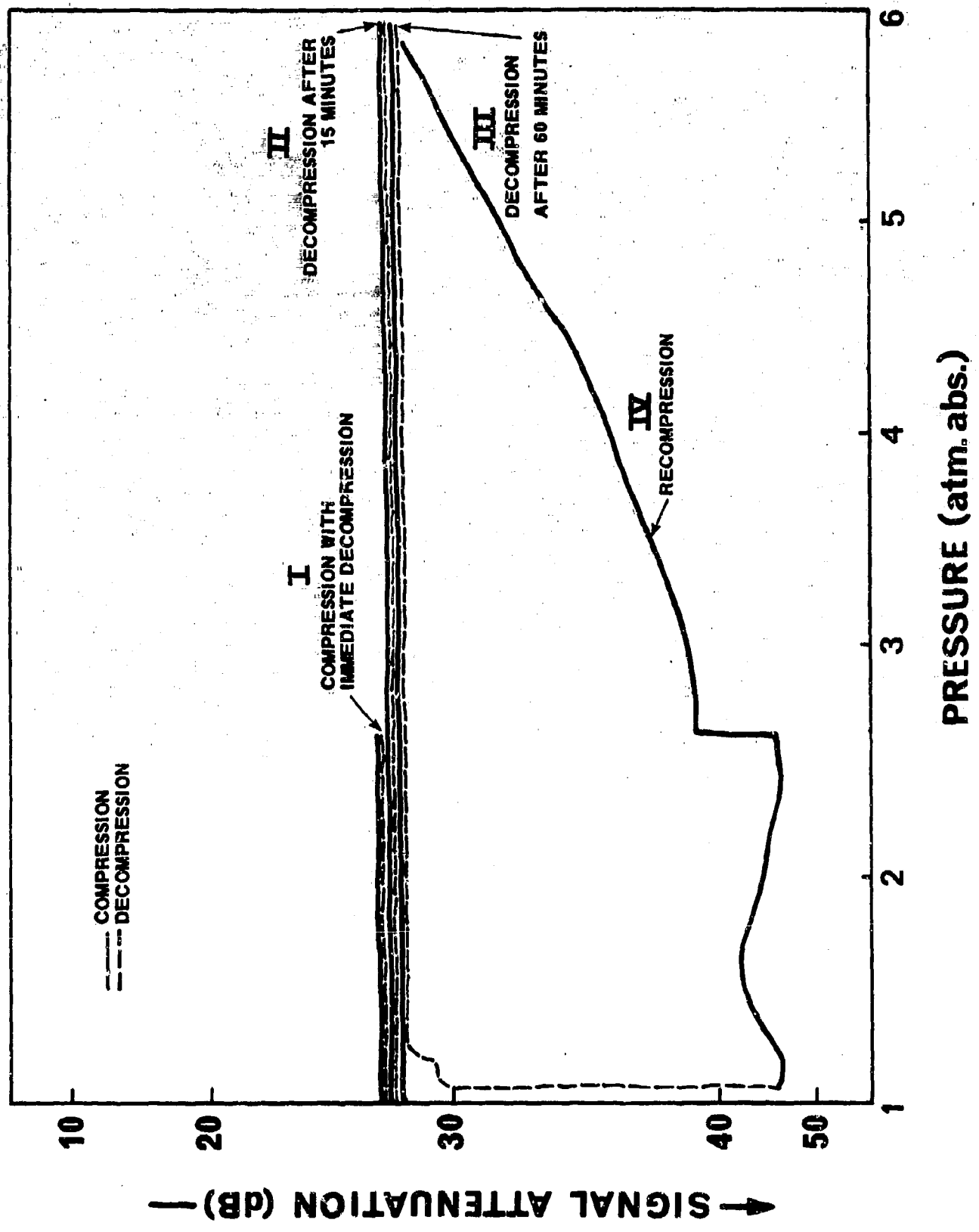
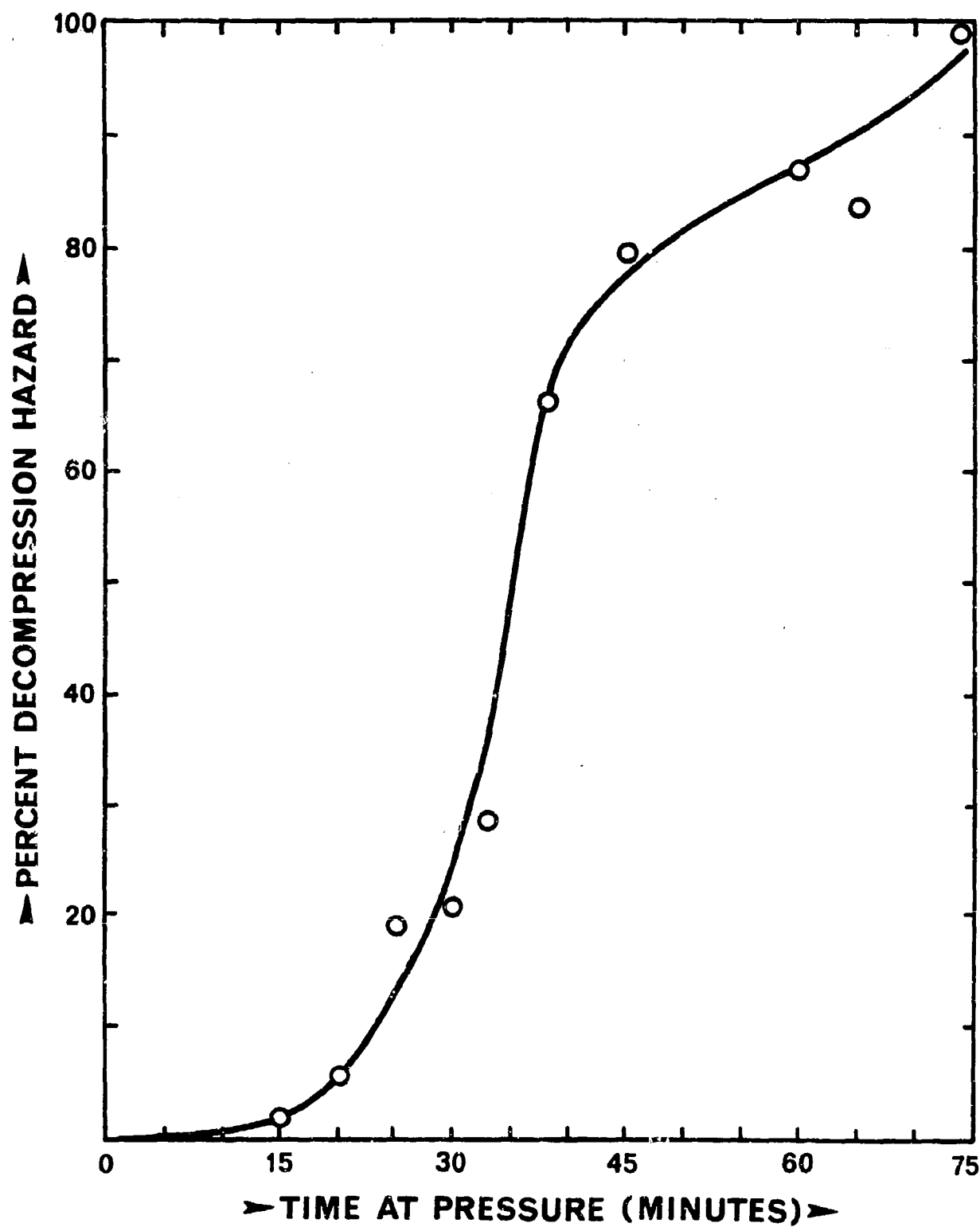




Figure 11. Per cent decompression hazard vs. time at 6 ATA in air. Decompression hazard is the sum of the bends score for the four rats divided by the maximum score of 24. (For explanation of bends score, see Table I).



easily detect bubbles in the extremities, there was usually no attenuation during the decompression stage itself, and there was a "lag period" of from 15 sec. to 2 min. after reaching 1 ATA before an attenuation was noted. In only 2 cases was an attenuation seen during the decompression stage.

#### D. Lag Period

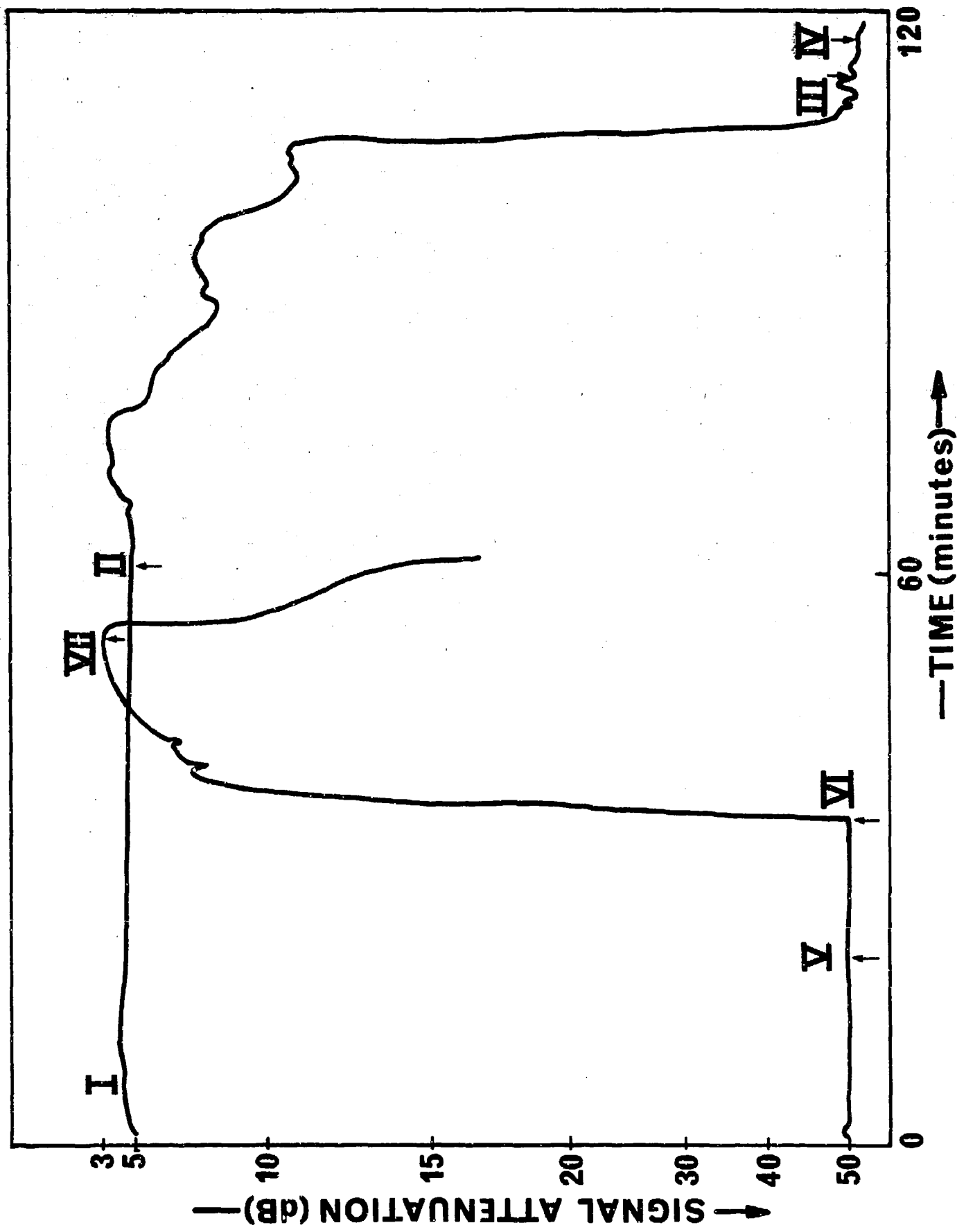
The monitoring technique described in B, above, was used to determine if bubbles could be detected in rats during stage decompression. Five rats were tested with profiles using short stops that were known to be inadequate (40 psi., 1 min.; 20 psi., 2 min.; 10 psi., 4 min.). No signal attenuations could be detected in the foot and all of the rats died. It was then decided that a check of the signal attenuation vs. time, rather than pressure, in conjunction with an observation of the circulatory system might give some indication of when bubbles were first making their appearance. This, it was hoped, would explain the "lag period" and the inability to detect an attenuation during stage decompression. In addition, an optical study of four anesthetized, surgically opened decompressed rats was made to determine the time of appearance of bubbles and possibly the locus of origin. The areas checked were the muscles of the thigh, the femoral vein and artery and its branches. Animals were compressed for a period of sixty minutes at a pressure of 6 ATA and then decompressed at 2 atm/min. to 1 ATA. Three animals were also monitored on the opposite thigh for signs of attenuation of an ultrasound beam. There was no visible evidence that bubbles were forming in the thigh muscle immediately

after decompression although evidence of this was given by the ultrasound attenuation. Larger bubbles in the circulatory system could not be seen until the animal had been at surface for several minutes. The small bubbles were either below the resolution of the microscope, or they could not be seen because of the translucent nature of the tissue. When bubbles were seen, and this occurred from ten minutes to fifty minutes after decompression, they were most common in the superficial epigastric vein and the muscular branch of the femoral vein. In one case, however, arterial bubbles were seen first.

In time, two of the animals were found to develop large bubbles in their veins and arteries and soon ceased to breathe although the heart had not yet stopped beating. Immediate artificial respiration was found effective in maintaining the animal until spontaneous respiration was resumed. This would indicate that the lung is still capable of gas exchange as the heart continues to beat and respiration is later again resumed. Central nervous system effects were evident in that the animal did not recover consciousness even after a period when the effects of anesthesia should have terminated.

The results of one such experiment with the transducers coupled to the thigh are shown in Figure 12; signal attenuation in decibels is plotted against time. At point I, the chamber was pressurized with air to 6 ATA and held for 60 minutes whereupon decompression at 2 atm/min (Point II) was begun. No bubbles were observed, and there was no signal attenuation shortly after reaching surface. After eleven minutes, a signal attenuation was found, and the signal strength decreased

Figure 12. Signal attenuation vs. time from start of compression. 5.7 MHz probes placed on the thigh muscles of a rat compressed to 6 ATA in air. (See text for details).



steadily for thirty minutes. Forty minutes after decompression, the signal strength fell precipitously, and soon arterial (III) and then venous (IV) bubbles were seen in the femoral artery and vein. At this point, the animal stopped breathing and was given artificial respiration. After twenty minutes, the animal began to breathe spontaneously (V) and he was returned to the chamber. Pressurization (VI) to 3.8 ATA caused an increase of signal strength to the initial predecompression value (within experimental error caused by the movement of the animal). Another decompression to 1 ATA (VII) again resulted in a decrease of signal strength.

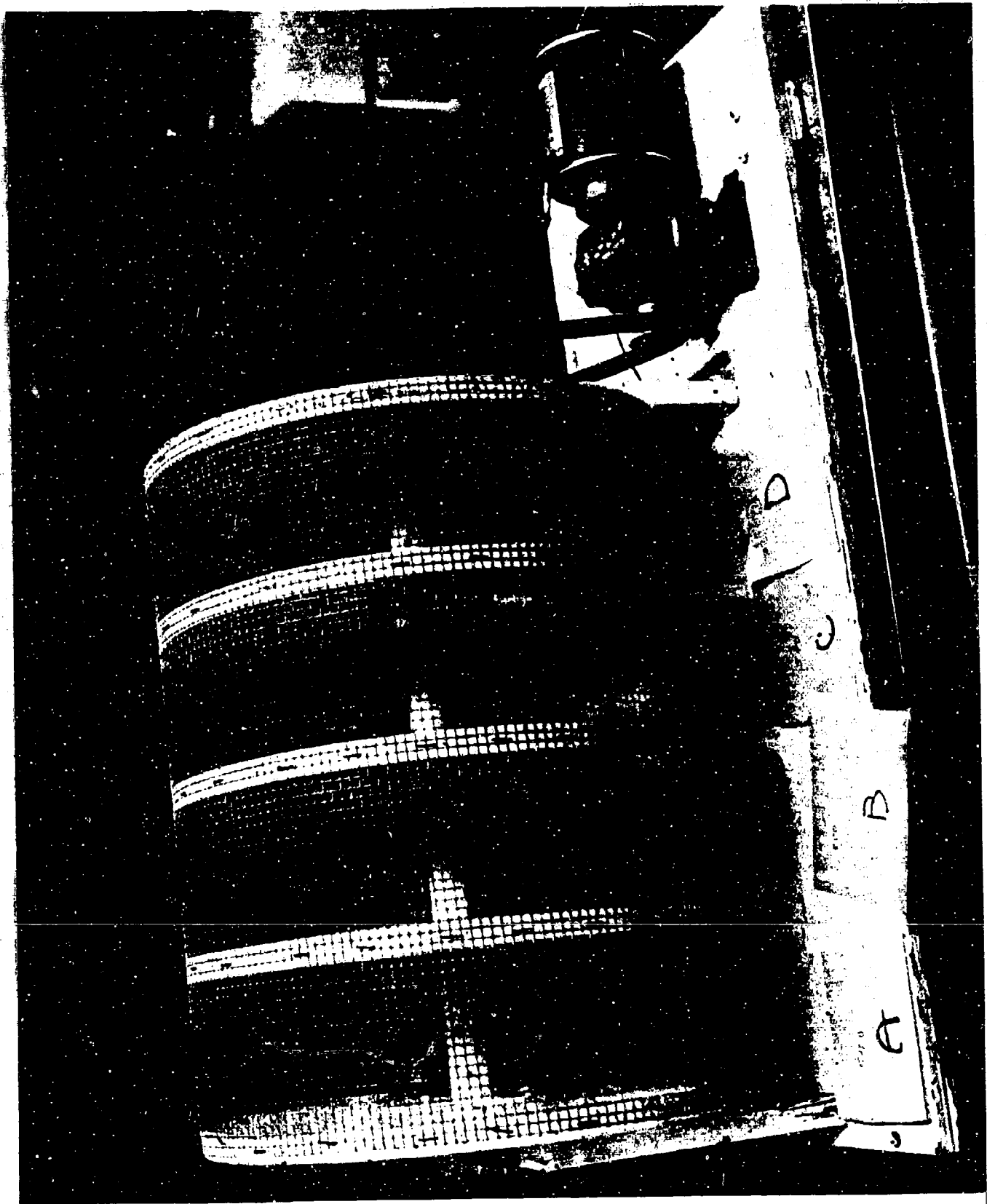
It was obvious from these experiments, noting signal attenuation vs. time, that bubble growth, in size and/or number, was a process which was slower than had first been anticipated. We then postulated that the development of symptoms of decompression sickness in the rat did not occur in a period following the appearance of bubbles, but rather paralleled the appearance of bubbles, and that this was a slow process.

#### E. Treadmill Study and Necropsy

To determine the time course for the development of decompression sickness in the rat and to assess the degree of distress, forty rats were compressed four at a time on air to 6 ATA for various periods ranging from 15 to 75 minutes, decompressed at 2 atm/min., and placed on a slow treadmill (1.8 m/min.), Figure 13, to be scored for the degree of severity of decompression sickness signs and their time of appearance. The scoring system is similar to that developed by Philp and

Figure 13. Treadmill used to assess the degree of decompression sickness in the rat. Speed is 1.8 m/min.





Gowdey (1964) and is given in Table II; the time course for development of these signs is shown in Figure 14. The individual scores for each rat are given in Table III.

It is clear that decompression sickness generally develops in a pattern in the rat. The longer exposures to pressure result in shorter "lag periods" for the development of distress signs and an increase in the severity of distress. For animals exposed to pressure for periods greater than 40 minutes, death can ensue without the development of paralysis. The animals first develop pain in the hind leg and then suddenly begin to show total loss of coordination and respiratory distress; death follows shortly thereafter.

Following the thirty minute scoring period, the rats were sacrificed with chloroform and a necropsy conducted to determine the number and site of bubbles. Of those animals which died of decompression sickness, arterial bubbles were always found. However, we were unable to observe good correlations of the severity of signs with the number of venous bubbles; indeed in one animal numerous bubbles were found in its posterior vena cava, but it did not exhibit decompression sickness signs other than increased breathing.

Bubbles were found in some locations more frequently than in others. They were rarely seen in the femoral vein until it was joined by the muscular branch. With great frequency, bubbles could be found in the superficial epigastric vein. Bubbles were seldom found in veins of the mesenteries.

TABLE II

Scoring protocol for decompression sickness signs

0	=	No visible signs, rats turn around in cages in treadmill
1	=	Slight, but noticeable, gait disturbances; walks only in one direction
2	=	Stiffness of hind limbs; appears to be "crawling" on front limbs
3	=	Dragging of hind limb
4	=	Complete paresis of hind quarters, rat can use only the front limbs
5	=	Complete front and hind limb paralysis
6	=	Death

TABLE III

Individual bends scores for various pressure exposures

<u>Time at Pressure (min.)</u>	<u>Individual Scores</u>	<u>% Decompression Hazard</u> *
15	1/2, 0, 0, 0	2%
20	1/2, 1/2, 1/2, 0	6%
25	2, 1, 1, 1/2	19%
30	2, 1, 1, 1	21%
33	2, 2, 2, 1	29%
38	6, 5, 3, 2	66%
45	6, 6, 5, 2	79%
60	6, 6, 6, 3	85%
65	6, 6, 6, 2	83%
75	6, 6, 6, 6	100%

Individual score divided by maximum possible score, X 100.

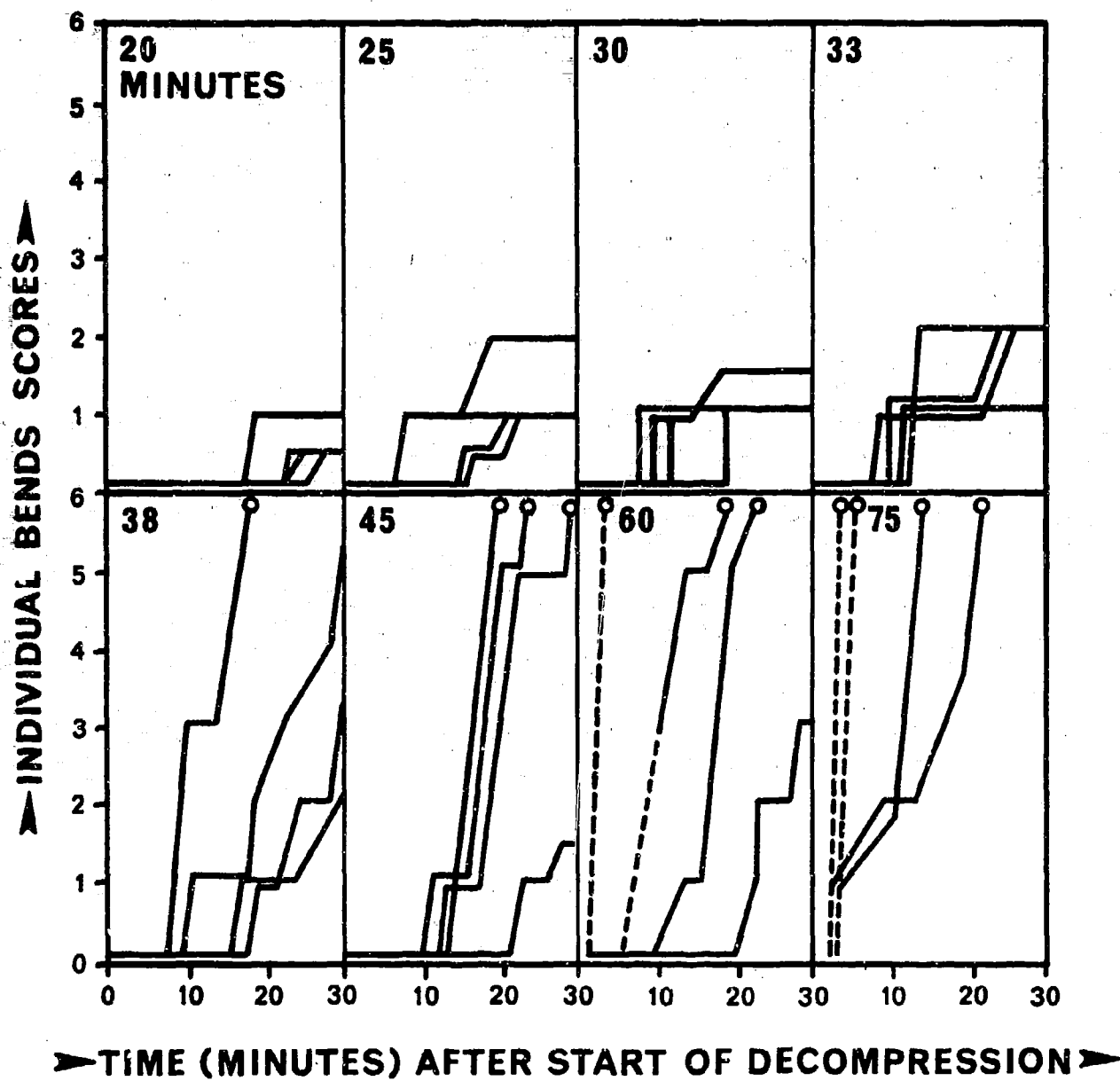


Figure 14. Bends score for each of 32 rats as a function of time from the start of decompression. All pressurizations made to 6 ATA in air; the "bottom time" is indicated in the upper left corner of each box.

#### F. Ultrasound Monitoring

Experiments were then conducted to determine the time course for the development of attenuations. From the results of the initial experiments with the hand and foot, the evidence is that attenuation is caused by bubble formation. These measurements were made on the thigh muscle at a frequency of 5.7 MHz, and only the intensity of the first transmitted signal was used. (Because the path length was greater though the thigh than the foot, it was possible to read the primary pulse). The animals were tranquilized with Acepromazine.

Recordings were made of the signal strength at the receiving transducer as a function of time after the start of decompression. These are shown in Figure 15 for 14 exposures to 6 ATA pressure for periods of 30, 40, 60, and 75 minutes. The circle at the ends of certain lines indicates that the subject died at this point. The arrow near the origin (start of decompression) of the abscissa marks the time of reaching 1 ATA or "surface".

Small motions of the rat's leg were not found to be particularly bothersome even though there often was quite a bit of movement. So far, we have not devised a method whereby the probes can be removed and reproducibly replaced with no change in signal strength. Such a technique would be of value not only in animal experiments but for the monitoring of human divers as well.

#### G. Long Term Monitoring

A small but more detailed study was made on rats which had been decompressed after a 40 minute exposure to 6 ATA. The increase and decrease in number of bubbles in the posterior vena cava as a function

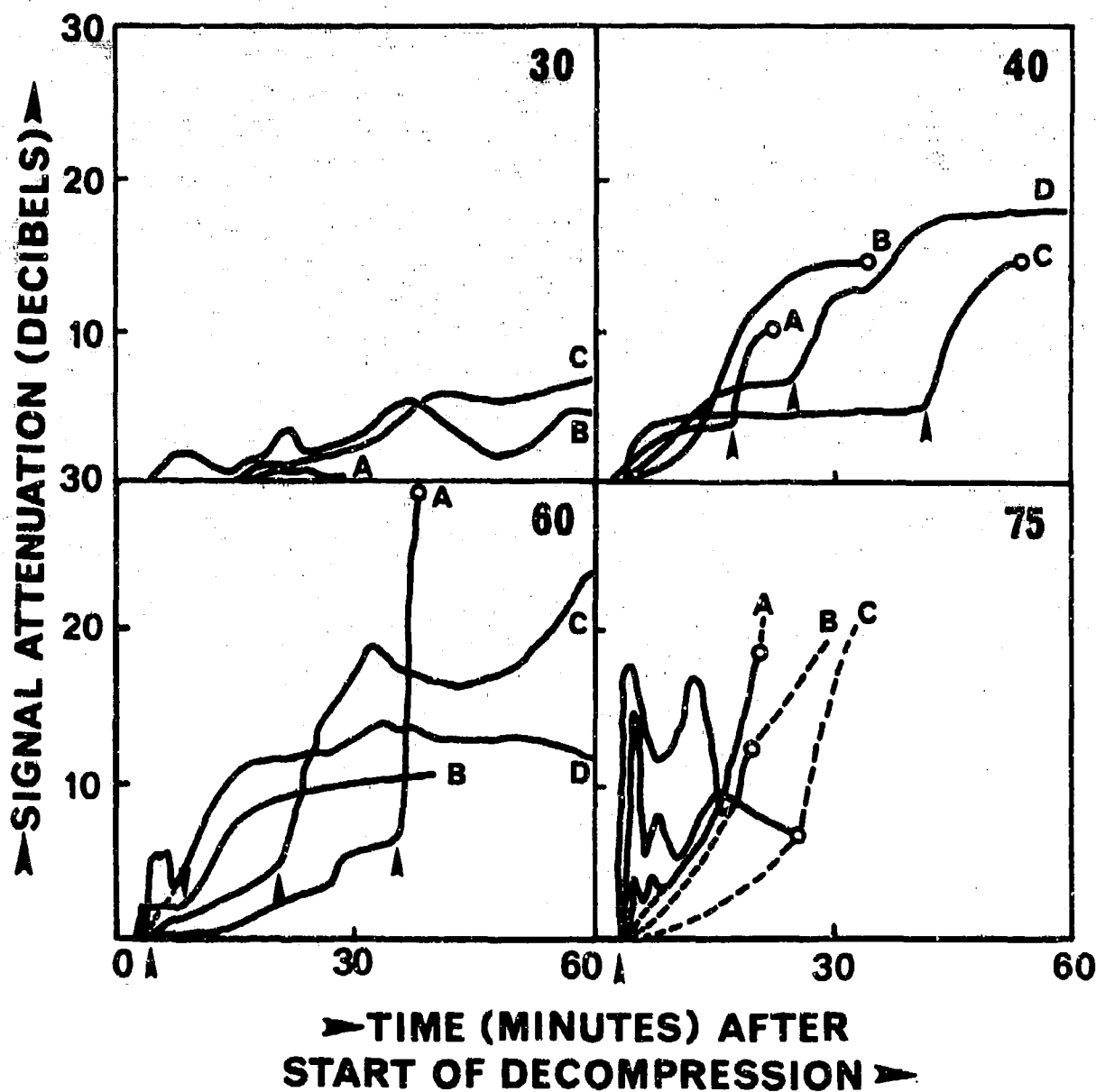


Figure 15. Attenuation of a 5.7 MHz signal measured across the thigh muscle as a function of time following start of decompression. All pressurization were made to 6 ATA in air; "bottom time" is indicated by the number in the upper right corner of each box.

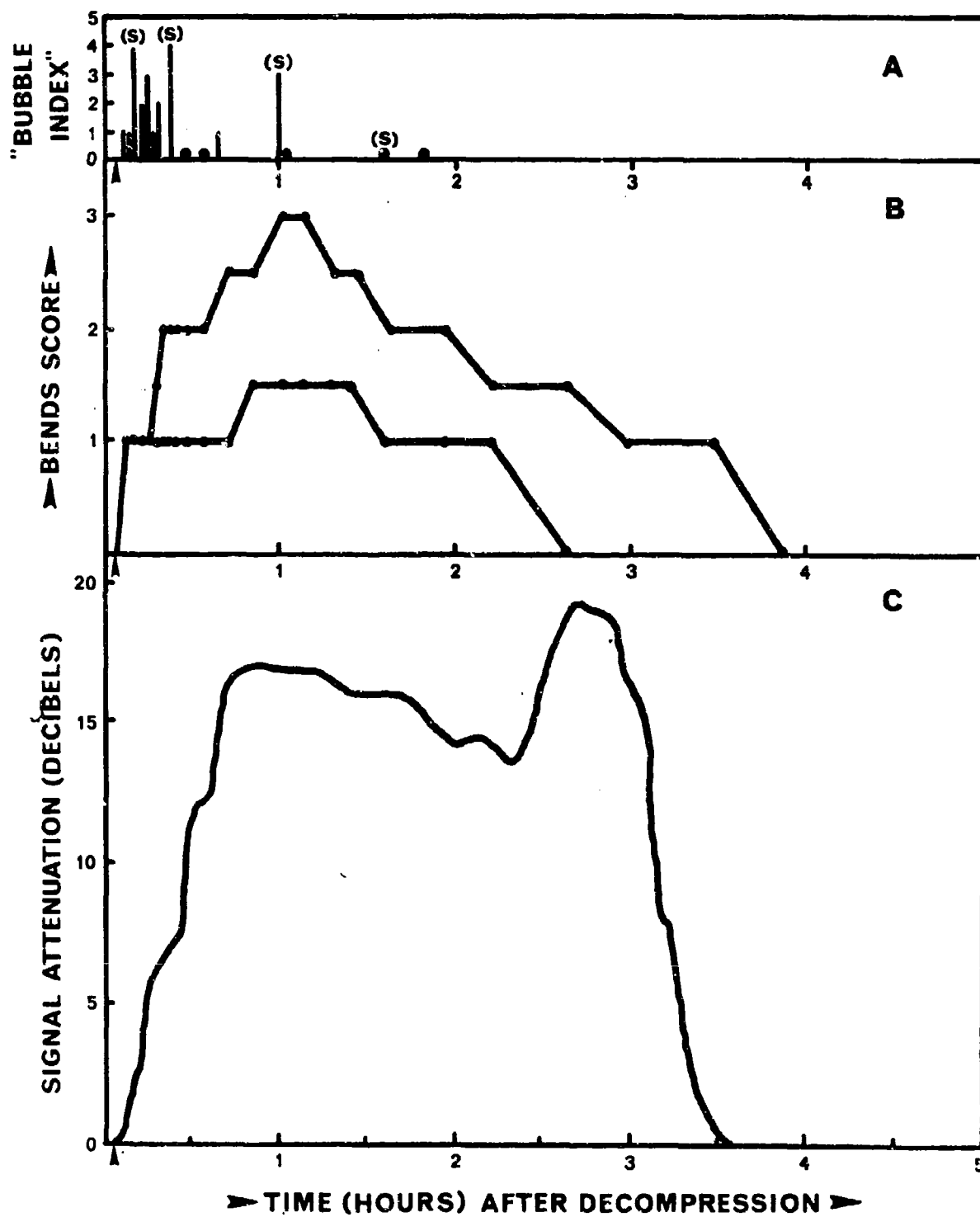
time was studied by sacrificing 16 rats with chloroform at various times after reaching 1 ATA. A necropsy was then performed, and the number and size of the bubbles visible to the unaided eye were noted; the results are shown in Figure 16A, plotted against an arbitrary index. Those bars marked with (s) represent the "index" of large rats which displayed signs of severe decompression sickness and had some difficulty in moving the hind limbs. Even in the rats with severe decompression sickness signs, we could not find evidence of bubbles in great vessels after a period of 1 1/2 hours.

Four rats were then compressed to 6 ATA, held, and decompressed and put on the treadmill. This was operated for a period of 1 to 2 minutes at a time to assess the gait of the animals, and the observations were carried out over a 4 hour period. The results of the experiment are shown in Figure 16B; two of the rats died before one hour (bends score = 6, not shown in Figure). It was difficult to determine the "end point", or return to the "normal" state, with any degree of exactness. Nevertheless, it should be noted that the effects of decompression last for a period of several hours, perhaps even longer than indicated on the graph.

A long-term ultrasound monitoring experiment was made with rats compressed and decompressed on the above-stated profile with the results indicated in Figure 16C. Of the seven rats tested, three died before one hour, and three showed only a small attenuation lasting but an hour. This was interpreted as indicating only slight decompression sickness for the latter case. For one of the rats, however, an attenuation of about 16 decibels was found and this is the experiment indicated in the figure.

- Figure 16 A. Bubbles detected visually in the posterior vena cava vs. time after decompression. "Bubble Index" is an arbitrary rating where "0" indicates no bubbles found and "5" indicates the most number of bubbles found. Bars with an (s) were rats which displayed severe signs of decompression sickness. Filled circles indicate an "Index" of zero. 6 ATA, 40 min., air.
- B. Individual bends score for two rats vs. time following start of decompression. 6 ATA, 40 min., air.
- C. Signal attenuation vs. time following start of decompression. 6 ATA, 40 min., air.





We found that long term measurements of this type are difficult to do with respect to finding rats that develop severe symptoms and yet eventually do not die. Work is in progress to develop a method whereby the probes can be applied and removed several times and still retain a stable baseline. This will allow us to monitor, over a long period of time, rats which have been shown to have decompression sickness.

## VI. DISCUSSION

In that it is not yet possible to measure ultrasonically the presence of small gas bubbles in the tissues of moving rats, the chief method employed in this study has been a comparison of the time courses for bends signs development and bubble development. In the initial phase of our study, we had expected to detect bubbles during the decompression phase of the experiment, that is, when a "metastable limit" had been exceeded. However, signal attenuations were never detected until some time after reaching "surface". This "lag period" was also found for the development of bends signs in the rat. Whether this inability to detect signal attenuation during and immediately after decompression represents a delay in phase separation, or whether it simply is the result of bubbles in a concentration below the detectable limit is not known at this time.

Figure 14 shows that there is a time after reaching surface in which no signs of distress can be observed. The shorter the exposures to pressure, the longer is this period. As the time at pressure increases, the "latency period" decreases and the severity of the signs increases. Rats which exhibit paralysis of the hind limbs (score 3 and 4) generally died although some recoveries were observed. Those animals which quickly develop severe paralysis died soon afterwards. In those animals which did not exhibit severe decompression sickness signs, death could ensue without the appearance of paralysis as a premonitory sign. After decompression, respiration rates often increased and this was more pronounced for rats with longer pressure exposures; it was more noticeable 5 to 30 minutes after decompression than 1/2 to 1 hour later.

In Figure 11, the "Decompression Hazard" for various times of pressure exposure showed a sharp rise in the range of 35 to 40 minutes. This rise, however, was not the result of an increasing severity of leg pain or paralysis but was rather a reflection of the increased number of animals which died (score 6). For animals decompressed from pressure to 1 ATA, paralysis of both back legs was generally noted as the most severe sign which could persist for any period of time with a remission following. After back leg paralysis, death was usually the next sign in the increasing severity of symptoms; arterial bubbles were found and often in great numbers. So far, death has not been observed by us in rats which did not contain some arterial bubbles after a decompression from increased pressure to 1 ATA. Rats were found which contained arterial bubbles and were not dead; thus arterial bubbles appear to be a necessary but not sufficient reason for death in the rat. We are therefore led to the conclusion that bends pain (here indicated by dragging of hind legs) and decompression death appear to be two separate and possibly different mechanisms, and the attempt to increase the severity of signs by increasing the exposure to pressure will be found to result in a bimodal distribution with death (score 6) increasing while the slighter symptoms (score 2 and 3) decrease. This can be seen in Table III.

The time of appearance of bubbles in the leg muscle of the rat is found to have a small "lag period" for all but the severest 75 minute pressure exposure (Figure 14). The growth of bubbles in the thigh muscle area, in size and/or number, can be seen to be a process with a time course of many minutes as shown in Figure 15. This compares with the time course for the development of decompression sickness signs indicated in Figure 14.

The degree of decompression problems in rats exposed to pressure for 30 minutes was slight and this is compared with the moderate increase of attenuation of the ultrasound beam; the attenuation varied from one to about seven decibels. The time course for the rise in ultrasound attenuation also can be seen to be long as it takes about 40 minutes for one case (curve B) and more than 60 for another (curve C).

Observations of animals on a treadmill (Figure 14) indicate that the degree of bends problems is more severe for animals on going from 30 minutes to 40 minutes to 60 minutes at pressure (there are a greater number of deaths also). This is in accordance with the degree of ultrasound attenuation (Figure 15) increase which also shows a change on going from 30 minutes to 60 minutes. The amount of attenuation does not exceed 5 to 7 dB for the 30 minute exposures, for the 40 minute exposure the range is about 5 to 18 dB, and for the 60 minute exposure to pressure the range is about 10 to 24 dB.

For the case of the 75 minute pressure exposures, the attenuation rise is comparatively rapid, although still with a time course taking many minutes. The initial peaks are possible caused by larger bubbles in the veins. This is suspected from the rapid changes of increase and decrease of the attenuation of the ultrasound beam. The dotted lines beneath the "peaks" are extrapolated curves to the region of the origin to indicate the supposed muscle-bubble attenuation, excluding the effects of venous bubbles. The time course for this rise is somewhat greater than that for the 60 minute pressure and is comparable to the time course for the development of distress signs shown in Figure 14 for 75 minute exposures to pressure.

At various points on the attenuation curves, sharp changes in slope were noted; these are seen in Figure 15 at 40 minutes (A, C and D) and 60 minutes (A, B and C). These rises are indicated by the small arrows. During the steep rise, signs of respiratory problems were often observed followed by death. The cause of this rapid rise, followed by death, is not yet known and may be the result of bubbles entering the femoral artery. The sharp rises would thus indicate the general presence of arterial bubbles, some of which could travel to the central nervous system with ensuing death.

Another explanation for the rise could lie with some mechanism which "triggers" the growth of nascent bubbles; many of these bubbles could then enter the venous system, and this was observed on one occasion when a rat was surgically opened to reveal the vena cava. The numerous venous bubbles could then break through the barrier of the lung circulatory system and enter the arterial system causing central nervous system embolisation.

Attempts to produce bubbles, and a resulting attenuation, by the application of intense ultrasound were unsuccessful. This was done by pressing the water-coated tip of a 300 watt ultrasonic disintegrator (Sonatron, Ultrasonic Devices, Inc.) to the thigh muscle. Little success was had in attempting to cavitate the blood in the vena cava, also.

Bubbles in the venous system in our experience are almost without observable effect. From the curve in Figure 16A, it can be seen that bubbles detected visually in the vena cava (after 40 minutes at 6 ATA are most prevalent in size and number about 10 to 20 minutes after the start of decompression. This is contrasted with the time course for the appearance and duration of decompression sickness signs (Figure 16B).

The long-term recording of the degree of attenuation persists for several hours and is comparable with the persistence of rear leg distress signs. The "peak" in the attenuation (curve 16C) and the bends-pain signs (curve 16B) both occurred about one hour after decompression. Thus the time courses for leg muscle embolization and leg pain are found to follow quite closely in the limited data we have at this time.

From the results of the necropsy studies and the studies of bubble appearance and persistence, we believe that there are several effects produced in the rat by a gas phase resulting from decompression. The time course for effects of decompression, i.e., pain and paralysis, persist in parallel with the time course for the presence of a gas phase in the tissue in question, i.e., the leg. There is, therefore, no need to involve biochemical mechanisms to explain the delay of onset of symptoms after decompression or of symptom persistence.

We have developed a working hypothesis in which bends pain and paralysis are the result of the growth in size and number of bubbles formed in the microcirculatory system of tissues (we designate these as Type I Figure 17). These bubbles grow in place ("thrombus-like") and do not circulate and later become trapped ("embolus-like"). They most likely do not arise de novo but rather grow from other nuclei already present on the walls of the vessels (Evans and Walder, 1970). These bubbles would then occlude the vessels with a resulting ischemia and tissue anoxia. While the mechanism of anoxic pain is not understood, it is possible that differences in ischemia between tissues may be the cause as is postulated by Salwan et al. (1968) for angina pectoris. In cases of paresis, the rat does not appear able to feel pain in the paralyzed limb. The rat will not

struggle or squeal when its paw is pinched or prodded with a sharp instrument.

Bubbles which grow and move into the venules and veins (Type II) are thus expected to be essentially functionless with respect to pain. They are most likely responsible for the increased respiration rate as they would be expected to cause reflex responses in the lung. These bubbles appear to be in veins draining some areas (e.g., the superficial epigastric vein) more often than others. Released bubbles from all parts of the body would therefore "pool" in the vena cava. Some areas or tissues might be able to tolerate a high degree of gas phase present without ill effects; bubbles would also be expected to be in the veins coming from these tissues and pass ultimately to the vena cava. This could explain why bubbles are always detected with a Doppler flowmeter in marginal decompressions of sheep, but signs of distress are usually not observed (Smith and Spencer, 1971).

Finally, decompression death in the rat appears to be the result of arterial bubbles (Type III) which causes an embolization of the blood vessels to the central nervous system. The result is a cessation of breathing with resulting suffocation and death. The method whereby bubbles can "pass through" the barrier of the lung is not yet known however. Observations by Spencer and Campbell (1968), using the Doppler Ultrasound flowmeter, have also shown that sheep expire after the appearance of arterial bubbles. They attributed these bubbles to the inability of the lung to serve as a filter if it becomes overloaded by too many venous bubbles, although Smith (1966) proposed that bubbles appear in arteries



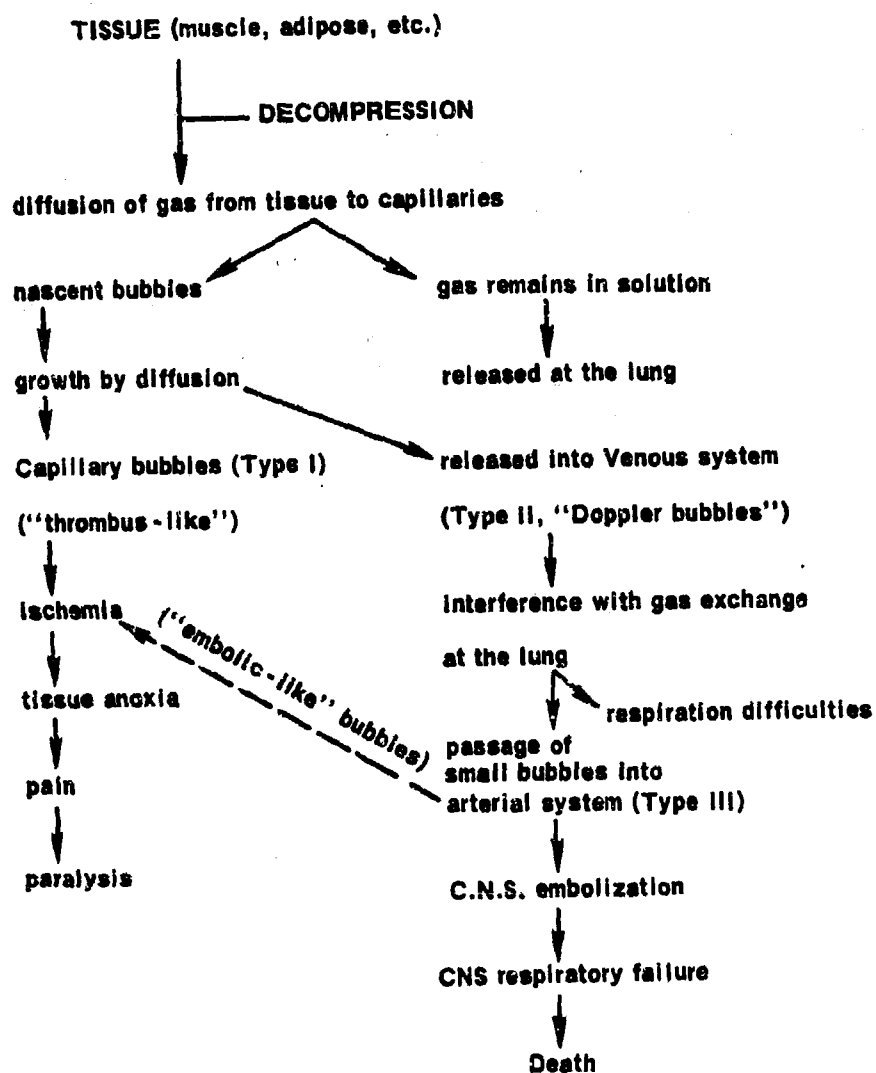


Figure 17. Working hypothesis indicating the location and pathophysiological result of each of the three types of bubbles.

before veins. In that obese rats would be expected to contribute many bubbles from adipose tissue into the venous "pool", as a class they would be expected to exhibit "decompression death" more than lighter rats; this was found by Saltee and Adams (1970). The results and hypothesis are summarized in Figure 17. Not all tissue types are expected to produce pain if a gas phase is present, e.g., adipose tissue.

Using the attenuation produced by the gas phase as a measure, it is of some interest to attempt to estimate the number of bubbles present in the muscle of the thigh. From Equation 10 we can calculate that, for a bubble whose radius is equal to the capillary radius ( $R_0 = 4$  microns), the attenuation coefficient is equal to  $7 \times 10^{-7}$  (nepers/cm) for each bubble. The coefficient is a constant within a factor of two for bubbles  $0.3 < R_0 < 7$  microns. For the case of mild bends signs, the increase of attenuation caused by bubbles is about 0.4 [nepers/cm], and the number of bubbles,  $R = 4$  microns, is thus  $6 \times 10^5$  [bubbles/cm<sup>3</sup>]. The number of capillaries in gracilis muscle (Martin, et al., 1932) is  $3 \times 10^6$  [cm<sup>-3</sup>] and in gastrocnemius muscle (Schmidt-Nielsen and Pennycuik, 1961)  $1 \times 10^6$  [cm<sup>-3</sup>] assuming a 500 micron capillary length. Thus the number of bubbles and the capillary number are approximately equal on the basis of this simplified analysis. Until an accurate figure for the bubble size is found, however, it will not be possible to determine the number of bubbles with any degree of accuracy.

VII. REFERENCES

- Barthelemy, L., (1963). Blood coagulation and chemistry during experimental dives and the treatment of diving accidents with Heparin, p.46, In: Proceeding Second Symposium on Underwater Physiology, National Academy of Sciences - National Research Council, Washington, D.C.
- Behnke, A. R., (1951). Decompression sickness following exposure to high pressures. Chap. III, In: Decompression Sickness, J. F. Fulton (ed.), W. B. Saunders, Philadelphia.
- Bert, P., (1943). Barometric Pressure. Researches in Experimental Physiology. Hitchcock, M. A., and F. A. Hitchcock, (trans.), College Book Company, Columbus.
- Blinks, L. R., V. C. Twitty and P. M. Whiteker, (1951). Part II. Bubble formation in frogs and rats, p. 145, In: Decompression Sickness. J. F. Fulton, (ed.), W. B. Saunders Co., Philadelphia.
- Boycott, A. E., G. C. C. Damant and J. S. Haldane (1908). The prevention of compressed air illness. J. Hyg. Lond., 8:342.
- Boyle, R., (1670). New pneumatical experiments about respiration, Philos. Trans. 5:2011.
- Buckles, R. G., (1968). The physics of bubble formation and growth. Aerospace Med., 39:1062.
- Buckles, R. G. and C. Knox, (1969). In Vivo bubble detection by acoustic-optical imagining techniques. Nature, 222:771.
- Cockett, A. T. K., J. C. Saunders and S. M. Pouley, (1968). Treatment of experimental decompression sickness by Heparin alone. Aerospace Med. Assoc., Annual Meeting, San Francisco, Calif.
- Devin, C., Jr., (1959). Survey of thermal, radiation, and viscous damping of pulsating air bubbles in water. J. Acous. Soc. Amer., 31:1654.
- Dunn, F., P. D. Edmonds and W. J. Fry, (1969). Absorption and dispersion of ultrasound in biological media. Chap. 3, In: Biological Engineering, Vol. 9, H. P. Schwan (ed.), McGraw-Hill, New York.
- End, E., (1938). The use of new equipment and helium gas in a world record dive. J. Indus. Hyg., 20:511.
- Evans, A. and D. M. Walder, (1969). Significance of gas micronuclei in the aetiology of decompression sickness. Nature, 222:251.
- Ferris, E. B., and G. Engel, (1951). The clinical nature of high altitude decompression sickness, P. 4, In: Decompression Sickness, J. F. Fulton, (ed.), W. B. Saunders, Philadelphia.

- Franklin, D. E., W. A. Schlegel and R. F. Rushmer, (1961). Blood flow measured by Doppler frequency shift of back-scattered ultrasound. Science, 134:564.
- Fry, W. J. and F. Dunn, (1962). U trasound: Analysis and experimental methods in biological research. Chap. 6, In: Physical Techniques in Biological Research, Vol. 4, W. L. Nastuk (ed.), Academic Press Inc., New York.
- Gersch, I. and H. Catchpole, (1951). Decompression sickness: physical factors and pathologic consequences, p. 165, In: Decompression Sickness. J. F. Fulton, (ed.), W. B. Saunders Co., Philadelphia.
- Gillis, M. F., M. T. Karagianes and P. L. Peterson, (1968a). Bends: Detection of circulating gas emboli with external sensor. Science, 161:579.
- Gillis, M. F., P. L. Peterson and M. T. Karagianes, (1968b). In vivo detection of circulating gas emboli associated with decompression sickness using the Doppler flowmeter. Nature, 217:965.
- Goberman, G.L. (1968). Ultrasonics, Theory and Application. Hart, New York.
- Greenbaum, L. J. and E. C. Hoff, (1966). A bibliographical Sourcebook of Compressed Air, Diving and Submarine Medicine, Vol. III, Office of Naval Research and Bureau of Medicine and Surgery, Department of the Navy, Washington, D. C.
- Harvey, E. N., (1951a). Physical factors in bubble formation. p. 90, In: Decompression Sickness. J. F. Fulton, (ed.), W. B. Saunders Co., Philadelphia.
- Harvey, E. N. (1951b). Part I. Bubble Formation in cats. p. 115, In: Decompression Sickness. J. F. Fulton, (ed.), W. B. Saunders Co., Philadelphia.
- Hempleman, H. V., (1963). Tissue inert gas exchange and decompression sickness. p. 6, In: Proceedings Second Symposium on Underwater Physiology, National Academy Sciences - National Research Council, Washington, D. C.
- Hills, B. A., (1966). A thermodynamic and kinetic approach to decompression sickness. Library Board of South Australia, Adelaide.
- Hoff, E. C., (1948, 1954). A bibliographical Sourcebook of Compressed Air, Diving and Submarine Medicine, Vol. I, II, Office of Naval Research and Bureau of Medicine and Surgery, Department of the Navy, Washington, D. C.
- Litovitz, T. A. and E. Carnevale, (1955). Effect of pressure on sound propagation in water. J. Appl. Phys., 26:816.

- Malette, W. G., J. B. Fitzgerald and A. T. K. Cockett, (1962). Dysbarism: A review with suggestions for therapy, Aerospace Med. 33:1132.
- Manley, D. M. J. P., (1969). Ultrasonic detection of gas bubbles in blood. Ultrasonics, 7:102.
- Martin, E. G., E. C. Wooley and M. Miller, (1932). Capillary counts in resting and active muscles. Am. J. Physiol., 100:407.
- Minnert, M., (1933). On musical air-bubbles and the sound of running water. Phil. Mag., 16:235.
- Nims, L. F., (1951). A physical theory of decompression sickness, p. 192, In: Decompression Sickness, J.F. Fulton, (ed.), W. B. Saunders Co., Philadelphia.
- Philp, R. B. and G. W. Gowdey, (1964). Experimental analysis of the relation between body fat and susceptibility to decompression sickness. Aerospace Med., 35:351.
- Philp, R. B., C. W. Gowdey and M. Prasall, (1967). Changes in blood lipid concentration and cell counts following decompression sickness in rats and the influence of dietary lipid. Can. J. Physiol. Pharm., 45:1047.
- Powell, M. R., (1971). Detection of gas-liquid phase separation in tissues by through-transmission mode ultrasound. Biophysical Society, 15th Annual Meeting, Abstract No. WFM-H8.
- Richardson, E. G., (1958). The mechanism of cavitation. Wear, 2:97.
- Sallee, T. L. and G. M. Adams, (1970). Symptomatology of decompression sickness in male Sprague Dawley rats. Aerospace Med., 41:1358.
- Salwan, F. A., D. S. Leighninger and C. S. Beck, (1968). The genesis of angina pectoris. Dis. Chest, 53:197.
- Schmidt-Nielsen, K. and P. Pennycuik, (1961). Capillary density in mammals in relation to body size and oxygen consumption. Amer. J. Physiol., 200:746.
- Smith, E. B., (1966). Decompression experiments with various inert gases. Chap. 35, In: Underwater Physiology, Proc. Third Symposium. C. J. Lambertsen (ed.), Williams and Wilkins, Baltimore.
- Smith, F. D., (1935) On the destructive mechanical effects of the gas bubbles liberated by the passage of intense sound through a liquid. Phil. Mag., 19:1147.

- Smith, K. H. and M. P. Spencer, (1970). Doppler indices of decompression sickness: their evaluation and use. Aerospace Med., 41:1396.
- Spencer, M. F. and S. D. Campbell, (1968). Development of bubbles in venous and arterial blood during hyperbaric decompression. Bull. Mason Clin., 22:1.
- Sutphen, J. H., (1968). The feasibility of using pulsed ultrasound to detect the presence of in vivo tissue gas bubbles. Report No. 508, U. S. Naval Submarine Medical Center, 27 Feb.
- Walder, D. N., A. Evans and H. V. Hambleman, (1968). Ultrasonic monitoring of decompression. Lancet, 897, 27 April.
- Workman, R. D., (1969). American decompression theory and practice, Ch. 12, In: The Physiology and Medicine of Diving and Compressed Air Work, P. B. Bennett and D. H. Elliott, (eds.), Williams and Wilkins, Baltimore.